INVESTIGATION OF ANTICANCER PROPERTIES OF NOVEL MDM2 INHIBITORS

A Thesis Submitted to
the Graduate School of
İzmir Institute of Technology
In Partial Fulfillment of the Requirement for the Degree of

MASTER OF SCIENCE

in Biotechnology

by
Sefayi Merve ÖZDEMİR

July 2021
İZMİR

ACKNOWLEDGEMENTS

I greatly appreciate my supervisor Prof. Dr. Ali ÇAĞIR for his supports, encouragements and advices during my thesis experiences. He also contributed so much things into my life to continue my studies.

I am so glad to my family, especially my mother to support me during my life and this period. And also I would like thank my grandmother for her contribution to my growth.

I would like to thank my friends, Gizem Tuğçe ULU, Suğra Fatma ECEVİT, Esra BİLGİÇ, Edip Kemal SARDOĞAN, Tuğbanur KARAMANKAYA, Elif ÇAĞLAR, Seren KEÇİLİ and Mustafa ERDOĞMUŞ. They became my second family in Gülbahçe. They are always kindly, supportive for me.

I am also thankful to Yağmur Ceren ÜNAL, Seren KEÇİLİ, Mustafa ERDOĞMUŞ, Ece YAZICI and Tuğçe ERDEMLİ for sharing their times for my challenges in this period.

I would like to appreciate Salih Mehmet YILDIZ, because he shared knowledge about cell culture procedures with me.

I am thankful to specialists Özgür OKUR and Murat DELMAN for flow cytometry analysis in IZTECH-BIOMER.

I would like to thank you for Prof Dr. Kemal Sami KORKMAZ and Assoc. Dr. Gülistan ÖZÇİVİCİ for supplying cell lines studies in this thesis.

This study was supported by the research grant from The Scientific and Technological Research Council of Turkey entitled as “The Investigation of Anticancer Effects of Ezetimibe, Desfluoro Ezetimibe and Synthesis Intermediates on Cancer Cells” and numbered as 219S152.

ABSTRACT

INVESTIGATION OF ANTICANCER PROPERTIES OF NOVEL MDM2 INHIBITORS

Cancer is one major disease causing death worldwide. Current cancer treatments are not %100 effective to cure for patients, yet. Thereby, the synthesis and discovery of new therapeutics have been important to improve the survival period of the cancer patients. There are many strategies for synthesis of cancer therapeutics. One of the most important strategy for cancer treatment is the reactivation of p53. MDM2 is a negative regulator of p53 in cell, because it causes the inactivation of p53.

In this thesis, the anticancer and MDM2 inhibitory properties of ezetimibe, desfluoro ezetimibe and intermediates during ezetimibe synthesis (named as SM2-9) and a side product from the synthesis of benidipine (named as SM1) on prostate cancer (LnCAP, wild-type p53), breast cancer (MCF7, wild type p53) and uterus cancer (HeLa, wild type nonfunctional p53) cells were investigated. For this purpose, the cytotoxic, cytostatic and apoptotic properties of these compounds were determined.

Compounds SM2, SM3, SM4 and SM6 demonstrated cytotoxic effects, whereas compounds SM5, SM8 and SM9 had cytostatic effects on three cells. Compound SM7 had no effect on these cells, up to 100 μM concentration. Compounds SM1 had cytostatic effect on MCF7 cells, but it showed no activity on other cells. Compounds SM8 and SM9 had strong cytostatic activity. Thus, the apoptotic properties of these compounds were examined by caspases 3/7 activation and Annexin-V FITC assays. Besides, MDM2 inhibitor profiles of these compounds were investigated by fluorescence polarization assay. This study provides novel and potential molecules for drug discovery in cancer treatment.

ÖZET

YENİ MDM2 İNHİBİTÖRLERİNİN ANTİKANSER ÖZELLİKLERİNİN İNCELENMESİ

Kanser, dünya çapında ölüme neden olan önemli bir hastalıktır. Bu tedaviler henüz kanser hastaları için %100 etkili bir tedavi sağlayamamıştır. Dolayısıyla, bu noktada kanser hastalarının yaşam sürelerini uzatmak için yeni ilaçların sentezi ve keşfi önemli olmuştur. İlaçların tasarlanması ve sentezi için birçok strateji vardır. Kanser tedavisi için en önemli stratejilerden biri p53 proteinin reaktivasyonudur. MDM2, hücrede p53'ün negatif düzenleyici bir proteinidir,

Bu tezde, ezetimib, desfloro ezetimib ve sentez ara ürünlerinin (SM2-9 olarak adlandırılmıştır.) ile benidipin sentezinde oluşan bir yan ürün (SM1 olarak adlandırılmıştır.) prostat kanseri hücreleri (LnCAP, doğal tip p53 proteini), meme kanseri (MCF7, doğal tip p53 proteini.) ve rahim kanseri (HeLa, doğal tip p53 protein) hücreleri üzerindeki antiproliferatif etkileri ve MDM2 inhibe edici özellikleri incelenmiştir. Bu amaçla, bu bileşiklerin sitotoksik, sitostatik ve apoptotic etkileri belirlenmiştir.

SM2, SM3, SM4 ve SM6 bileşikleri üç hücre hattı üzerinde sitotoksik etkiler gösterirken, SM5, SM8 ve SM9 bileşikleri bu hücre hatlarında sitostatik etki göstermiştir. SM7 bileşiğinin 100 μM konsantrasyona kadar bu hücre hatları üzerinde hiçbir etkisi saptanamamıştır. SM1 bileşiği MCF7 hücrelerinde sitostatik etki göstermiştir, fakat diğer hücrelerde aktivite göstermemiştir. SM8 ve SM9 bileşikleri, güçlü sitostatik aktiviteye sahiptir. Bu nedenle, bu bileşiklerin apoptotik özellikleri kaspaz 3/7 aktivasyonu ve Annexin-V FITC testleri ile incelenmiştir. Ayrıca bu bileşiklerin MDM2 inhibitör profilleri floresan polarizasyon deneyi kullanılarak araştırıldı. Bu çalışma, kanser tedavisinde ilaç keşif araştırmaları için yeni ve potansiyel moleküller sunmaktadır.

To my grandmother Atike ÖZDEMİR

TABLE OF CONTENTS

LIST OF FIGURES

Figure **Page**

LIST OF TABLES

LIST OF ABREVIATION

DNA	Deoxiribonoucleic acid
p53	Tumor protein 53
SV40	Simian virus 40
MDM2	Murine double minute chromosome 2 gene
CDKN1A	Cylin-dependent kinase inhibitor 1A
p21	Cyclin dependent kinase inhibitor 1
CDK2	Cyclin-dependent kinase 2
CDK4	Cyclin-dependent kinase 4
E2F1	E2F transcription factor 1
CDK1	Cyclin-dependent kinase 1 encoding gene
PCNA	Proliferating nuclear antigen
Rb	Negative regulator of cell cycle
ATM1	Ataxia telangiectasia mutated kinase
GADD45A	Growth arrest and DNA damage inducible alpha
P53R2	p53 inducible ribonucleotide reductase gene

TNF	Tumor necrosis factor
TRAIL	TNF-related apoptosis-inducing ligand
BALB3t3dm	*Mus musculus* fibroblast cell line
BCL-X	BCL-2 associated X protein
BAK	BCL-2 antagonist/killer 1
PUMA	P53 upregulated modulator of apoptosis
BAX	Bcl-2-associated X protein
NOXA	Phorbol-12-myristate-13-acetate-induced protein
Smac	Second Mitochondria-derived Activator of Caspases
DIABLO	Direct IAP-Binding protein with Low PI
Apaf-1	Apoptotic protease-activating factor 1
HtRA2	HtrA Serine Peptidase 2
Caspase	Cysteine-aspartic proteases
DBB2	DNA damage-binding protein 2
Leu	Leusine aminoacid
Phe	Phenyl aminoacid
Trp23	Tryptophan aminoacid

TAFII31	Transcription initiation factor
TAFII70	Tanscription initiation factor TFIID subunt 6
TFIID	Transcriptin initiation factor II D
Gly	Glycine
Glu	Glutamic acid
Val	Valine
Cys	Cysteine
p300/CBP	CREB-binding protein transcriptionalcoactivator proteins
NLS	Nuclear localization signal
NES	Nuclear export signal
SPR	Surface plasmon resonance spectroscopy
K_d	Equilibrium dissociation constant
K_i	Equilibrium inhibitory constant
SJSA-1	Osteosarcome cell line
GI_{50}	Concentration at %50 maximal inhibition of cell proliferation
nM	Nano molar

μM	Micro molar
μL	Microliter
mP	Molar polarization
mL	Mililiter
MCF7	Breast cancer cell line
HeLa	Uterus cancr cell line
LNCaP	Prostate cancer cell line
Log P	Partition coefficient
Log S	Solubility

CHAPTER 1

INTRODUCTION

1.1. Cancer

1.1.1. Cancer Epidemiology

Cancer is multifactorial disease underlying many molecular mechanisms in cell. Cancer is originated from abnormal cell proliferation and resistance to mortality of cells. Cancer progression is generally resulted from DNA damage or mutations in proto-oncogenes that found in cell growth mechanisms and in tumor suppressor genes that are involved in the stimulation of cell growth and apoptosis. Up to now, it has been known that there are more than 200 cancer types in worldwide [1].

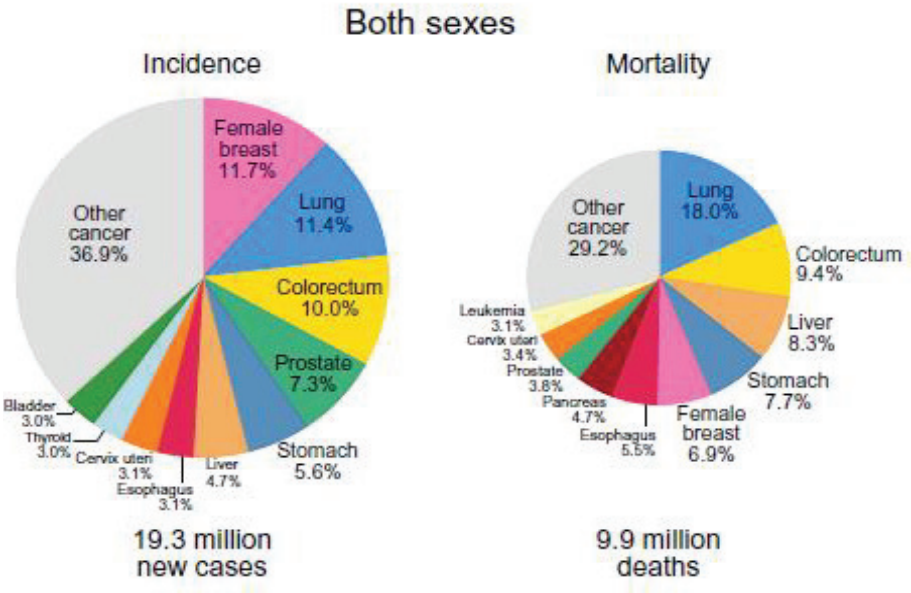

Figure 1.1. Cancer incidences and mortality ratios in 10 common cancer types for both sexes in 2020 [2].

Cancer is one of the major diseases having high mortality rates in world. According to GLOBOCAN (Global Cancer Statistics) results in 2020 that were produced by International Agency for Research on Cancer, it was estimated that 19.3 million new cases of cancer have been occurred, and approximately 10 million of cancer cases is ended with deaths. Among them, breast cancer in woman is most commonly diagnosed with 11.7 % incidence ratio. The most leading cause of cancer deaths are resulted from lung cancer. Lung cancer cases is estimated as 11.4% incidence with 1.8 million deaths. After lung cancer, colorectal, prostate and stomach cancers have high incidence rates as (10.0 %, 7.3% and 5.6% respectively). Cervical cancer is the most frequently seen in women, subsequently with 604,000 cases and 342,000 deaths. Followed by lung cancer, most seen cancer type in men is prostate cancer with about 1.4 million cases and 375,000 deaths [2].

1.1.2. The Leading Causes of Cancer

Cancer disease occurred due to the epigenetic and genetic mutations in cells. There are many physical and chemical factors associated with genetic and epigenetic changes. Genetic changes are resulted from carcinogenic agents, UV radiation, γ-radiation ionizing radiation, reactive oxygen species, viruses and aging, while epigenetic changes are caused from aging and chronic inflammation [3]. The reason of genetic alterations is DNA damage that is the first step of cancer development. Genetic alterations in human cancer types lead to mutations in proto-oncogenes and tumor suppressor genes. Mutations in proto-oncogenes result in the activation of oncogenes (gain-of-function) that are involved in cell division and survival, whereas they cause loss-of function in tumor suppressor genes that by inactivating them [1].

1.1.3. Cancer Cells

Cancer is a disease resulted from the unregulated growth of cells. The hallmarks of cancer cells are classified as genome instability, having no cell death program, distinctive energy metabolism, invasion, metastasis and angiogenesis. Unlike normal cells, cancer cells have no cellular degradation machinery for programmed cell death for aged and deformed cells, so they are able to continue to grow and divide infinitely. Cancer cells behave invasive, thus can spread whole body from their original sites. They are capable of forming cell mass and tumors in another body parts [4].

The other hallmarks of cancer that contributes the complexity of cancer mechanisms are being self-sufficient in growth factor signals and resistant to anti-growth factors. This cause limitless replicative property to cancer cells. In normal cells, cell cycle is strictly regulated depending on the growth signaling pathways for maintaining cell proliferation, whereas cancer cells having alterations in growth signaling pathways is suitable for their survival. Reprogramming processes in energy metabolism and evading immune response are also important hallmarks for cancer survival [5].

1.2. p53 Pathway in Cancer

1.2.1. p53 Tumor Suppressor Protein

p53 protein was firstly extracted from SV40 transformed rodent cells p53 is a tumor suppressor protein that is well- studied in cancer researches [6]. It is called as guardian gene of genome, because of its inducing cell cycle arrest, apoptosis, cell senescence and autophagy as seen in figure 1.3. p53 is a nuclear phosphorylated protein consisting of 393 amino acid residues [7]. P53 is a transcription factor that controls the expression of many genes that are mediating cell growth, division, survival and/or programmed cell death in unstressed cells. Under stress conditions, p53 expression is activated for maintaining cell cycle arrest, apoptosis, DNA repair mechanisms, cell senescence and autophagy [8]. p53 protein have five functional domains including transcriptional activation domain at its N-terminal, the proline-rich region, the DNA-binding domain, the oligomeric domain, regulatory domain at C-terminal which is sensitive to the proteasome as seen in figure 1.2 [9].

Figure 1.2. The structure of p53 protein.

p53 gene is high frequently mutated in many kinds of cancer. The loss of functional p53 protein in cells makes them immortalize, when the over-expression of p53 gene cause

cell cycle arrest and apoptosis. There are many mutations in p53 gene resulting in abnormalities in human cancers. In lung cancer, mutations in p53 have %50 frequency, and breast cancer have 30-86% frequency from whole genome mutations. In primary melanomas, %97 of all mutations belongs to p53 gene alterations [10].

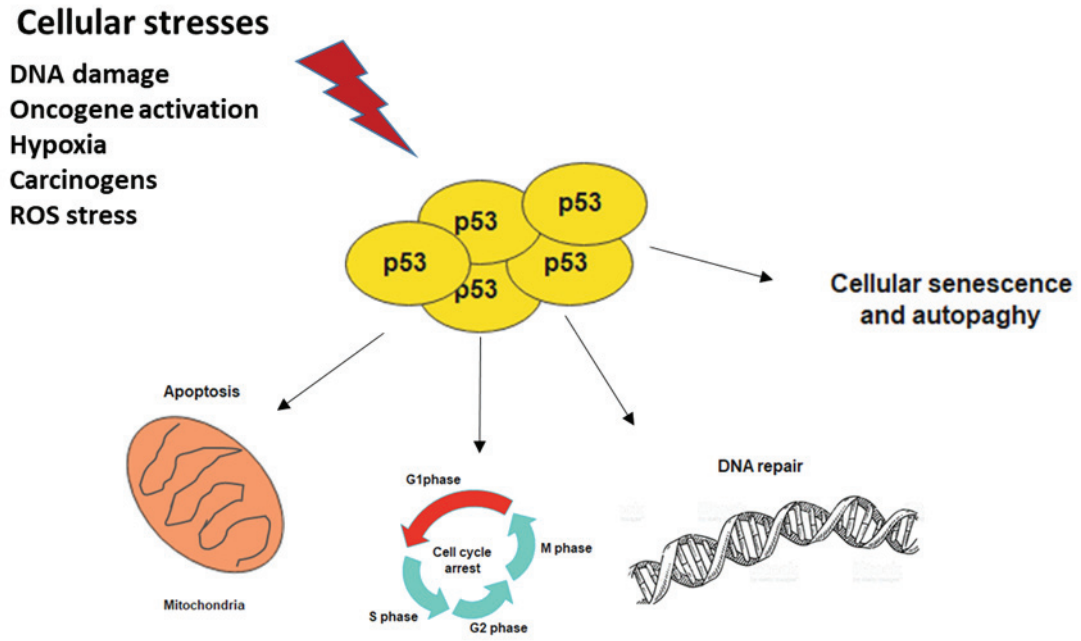

Figure 1.3. The p53 roles in cells under cellular stresses including apoptosis, cell cycle arrest, DNA repair, cellular senescence and autophagy.

The p53 pathway is responsible for the expression of many genes that are respond to many intrinsic and extrinsic signals that affect the cellular homeostasis. As response to stress, p53 becomes activated by post-translational modifications. p53 is essential transcription factor for many biological process in cell, so it is strictly regulated at both transcriptional level and post-translational level. In unstressed cells, p53 protein is continued at low level and is short-lived and rapidly degraded by MDM2 protein, comparing to stressed cells in which p53 protein accumulates and becomes active as transcription factor against to DNA damage, chromosome instability, nucleotide exhaustion and hypoxia or high ROS levels. The activation of p53 triggers the expression of more than 150 genes that are mediate the arrest of G1/S phase, the programmed cell death and other events [11]. Among these signals that are induce p53 activation is DNA damage. DNA damage is occurred by many physicals and chemical reasons including UV radiation, ionic radiation, base alkylation, ROS level

and depurination of bases. Each of types of DNA damage is perceived by different set of proteins in p53 pathway that alter p53 protein in different amino acid residues, by this way, the nature of stress signal is conveyed to p53 protein by post-translational modifications [12].

1.2.2. The role of p53 in Cell Cycle Arrest

Cell cycle arrest is accomplished by p53 that transcriptionally activates p21 and WAF1 genes. p53-induced WAF1 activation mediates growth inhibition by stimulating apoptosis in humans and rodents [13]. In figure 1.4., p53 can bind to p21 promoter at its upstream sites to activate p21 genes. Cyclin E/Cdk2 and cyclin D/Cdk4 protein complexes are inhibited by p21 to arrest G1 cycle. p21 protein inhibits Cdk2 and Cdk4 proteins to prevent pRb phosphorylation, so pRb can bind to E2F1 transcription factor. To promote the transcription of E2F1 provides the silencing of E2F1 target genes that are important for DNA replication and cell-cycle processes. Thereby, pRb protein suppress the transcription of genes that are required for G2/M progression. Luo et. al demonstrated that p21 is also related with PCNA (proliferating cell nuclear antigen) for blocking DNA replication in vitro.

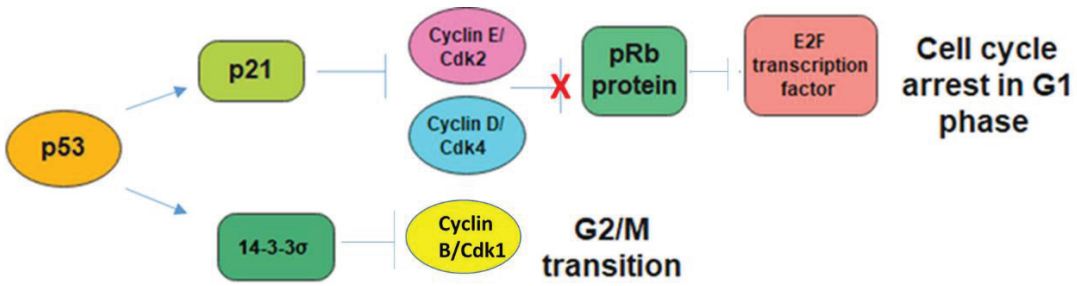

Figure 1.4. The role of p53 protein on cell cycle arrest at G1/S and G2/M checkpoint.

p53 is also play role in cell cycle arrest at G2/M phase. Whereas p21 dependent inhibition of cyclin B/Cdc 2 results in cell cycle transition to mitosis, 14-3-3σ gene that is p53 target, can contributes to block G2/M transition by cytoplasmic requisition of CDC2-cyclin B complex [14].In addition, after DNA damaging, cdc25C promoter is repressed by p53 to induce G2/M arrest. This p53-mediated cell cycle arrest is important for cell cycle checkpoint functions. When DNA double stranded breaks are occurred by ionizing radiation,

ATM (ataxia telangiectasia mutated) kinase becomes activated. ATM kinase inhibits MDM2 ligase activity by phosphorylating it leading to quickly accumulated p53 protein. This rapid accumulation of p53 protein in cell cause to the activation of p21. p21-mediated G1 arrest allows to time for repairing double-strand breaks. By this way, p53 achieves to control genome integrity and the survival of damaged cells [15]. According to study reported by Gatz et al. 2006, p53 maintains the transcription of many genes that have functions in DNA recombination and repair. p53 target genes such as GADD45 is a gene participating in chromatin remodeling to reach DNA damage and p53R2 is an enzyme that supply precursors for DNA repairs [16] p53 also controls post mitotic events such as blocking DNA re-replication when mitotic spindle is destroyed to provide chromosome stability [17].

1.2.3. The role of p53 in Apoptosis

Apoptosis is programmed cell death that is identified by distinct morphological and biochemical alterations. These changes are maintained by caspases. Two major apoptotic pathways are classified as intrinsic (mitochondrial) and extrinsic (death receptor) pathways. In extrinsic pathway, the cellular transmembrane receptors such as CD95, TNF receptor, and TRAIL binds to its ligand resulting in the recruitment of adaptor proteins including caspases 8 and 10. This event cause the activation or cleavage of effector caspases including caspases 3 and 7.

In intrinsic pathway, apoptotic stimulus induces mitochondria directly or indirectly by proapoptotic proteins that belongs to BH-2 family such as Bax, Bak, Puma and Noxa. Mitochondria can release apoptogenic signal to induce caspase activation, later. The intrinsic pathway includes the disruption of mitochondrial membrane and the liberation of mitochondrial proteins such as cytochrome c, Smac/DIABLO and HtRA2. Cytochrome c induces the activation of caspase 9 together with Apaf-1 to initiate caspase cascades including the activation of caspases 3, 6 and 7. Proapoptotic Bcl-2 family proteins Bax, Bak are directly activated by BH-3-only Bcl-2 protein Bid to achieve membrane permeabilization in mitochondria. The other BH-3 only proteins PUMA, Noxa binds to antiapoptotic proteins Bcl-2 and Bcl-Xl resulting in the activation of Bax, and Bak, alternatively. There is a crosstalk between two pathways, because caspase 8 induces proteotically activation of Bid protein that can provide cytochrome c release from mitochondria [18].

The role of p53 in apoptotic pathways firstly identified in murine myeloid leukemia cell lines having mutant p53. In cells, p53 activation induces apoptosis in response to stress. p53-dependent apoptosis is occurred by transcriptional activity of p53. Intrinsic pathway is activated by p53 under the stress such as DNA damage and hypoxia. In figure 1.5, p53 induces the transcription of proaopototic genes expressing Bax, Bak, PUMA and Noxa proteins, but it can suppress antiapoptotic Bcl-2 proteins such as Bcl-2, Bcl-XL and survivin (IAPs). In extrinsic pathway, p53 induces the transcription of CD95 and TRAIL receptor 2 (TRAIL-R2/DR5) to sensitize cells for extrinsic apoptosis [19].

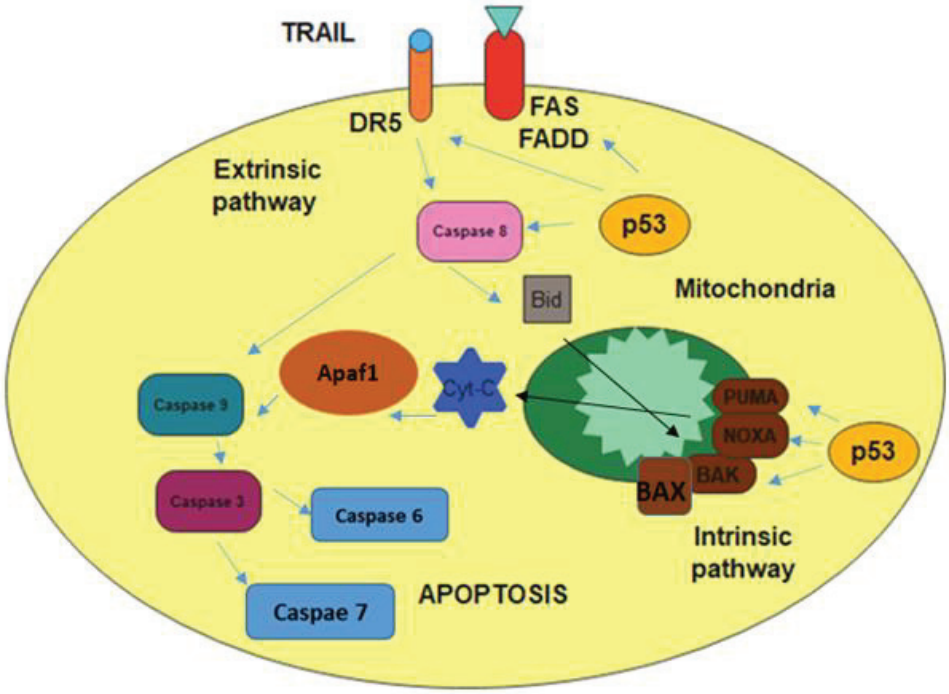

Figure 1.5. The representation of p53 role in apoptosis.

1.2.4. The role of p53 in DNA repair and cell senescence

Endogenous and exogenous factors caused DNA lesions are reverted by cells with sophisticated DNA repair mechanisms. There are three types of repair mechanisms in cells including nucleotide excision repair that removes helix-distorting lesions; base excision repair that corrects oxidative base modifications and mismatch repair that detect erroneously inserted nucleotides during replication [19]. P53 gene is important transcription factors for upregulating DNA repair genes such as Gadd45a, DBB2, XPC, p53R2, KARP-1 thymine DNA glycosylase and MGMT. The transcription-independent activities of p53 on DNA

repair facilitate protein-protein interactions with the helicases XPB and XPD that are repair proteins, DNA polymerase beta and the homologous recombination factor RAD51 [20].

1.3. MDM2-p53 Pathway in Cancer

1.3.1. MDM2 Oncoprotein

MDM2 is an oncogene that is discovered in murine double minute chromosome of BALB3t3dm cell line [21]. MDM2 gene (sometimes referred to as Hdm2) encodes a 491-amino acid polypeptide having a p53-binding domain, an acidic region, a ZINC-finger, and a RING-finger domain as shown in figure 1.6. MDM2 physically associates with p53 to control p53 level in cell. In the absence of cellular stress, there is an auto regulatory feedback loop for controlling p53 level. MDM2 functions in the inhibition of p53 activity by binding its transactivation domain and facilitating its proteasomal degradation. p53 also, regulates mdm2 expression at transcription level. The MDM2 has ubiquitin E3 ligase activity that ubiquitinates p53 for its proteosomal degradation in the elevated p53 levels. MDM2 can export p53 from nucleus to proteasome in cytoplasm for degradation [9, 22].

Figure 1.6. The structure of MDM2 protein.

1.3.2. MDM2-p53 Interaction

The first response to cellular stress is to immediately stabilize for p53 activation. The activated p53 can regulate transcriptional expression of many genes that function in cell cycle arrest, repair mechanisms and apoptosis. In normal cells, it is important to kept p53 level low by the rapid proteosamal degradation of p53. This degradation is done by both ubiquitin dependent and independent mechanisms that have many signaling pathways including various post-translational modifications of p53. Among these pathways, ubiquitinatination of p53 by MDM2 having E3 ligase activity is the most important one. MDM2 is primary regulator for p53 activation, besides several E3 and E4 ligase exist for p53 degradation. MDM2 is linked to p53 with auto regulatory negative feedback loop (as

shown in figure 1.7) to control low cellular p53 levels in unstressed cells. This negative feedback loop provides the upregulation of MDM2 via p53 led to control of the intracellular level of both proteins and check that p53 concentration remain low [23, 24].

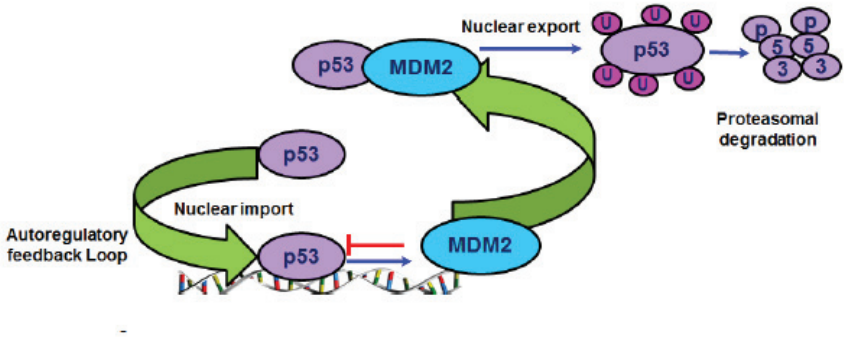

Figure 1.7. The auto-regulatory loop of p53-MDM2 complex [25].

1.3.3. The Structure of MDM2-p53 Complex

MDM2–p53 interaction is firstly identified by yeast-two hybrid and immunoprecipitation experiments. They interact through N-terminal domain of MDM2 with N terminal transactivation domain of p53. When MDM2 binds to transactivation domain, it inhibits the transcriptional activity of p53, directly. The crystallographic data of MDM2-p53 complex showed that MDM2 amino terminal domain constitutes a hydrophobic cleft into the transactivation domain of p53, thereby this conceals p53 this region from transcriptional machinery. MDM2-binding region of p53 consists of residues from1-41 or 1-52, whereas p53 binding domain of MDM2 has residues from 1-118 or 19-102. According to site-directed mutagenesis, there were important key residues on p53 including Leu14, Phe19, Trp23, Leu22 and Leu22 for their interaction, but most critical ones are Phe19, Trp23 and Leu26. These residues can also contact with human TATA-binding protein (TBP) associated factors TAFII31 and TAFII70 in TFIID; these contacts are needed for p53 transcriptional activity. The direct interaction between p53 and MDM2 is required quite small (25-109 aas) hydrophobic pocket domain at amino terminal of MDM2 and an amphipathic peptide (15 aas) at amino terminal of p53. The minimal binding-site of MDM2 on p53 is within residues 18-26. It was observed that mutations in MDM2 binding site results in a resistance in p53 proteasomal degradation [26].

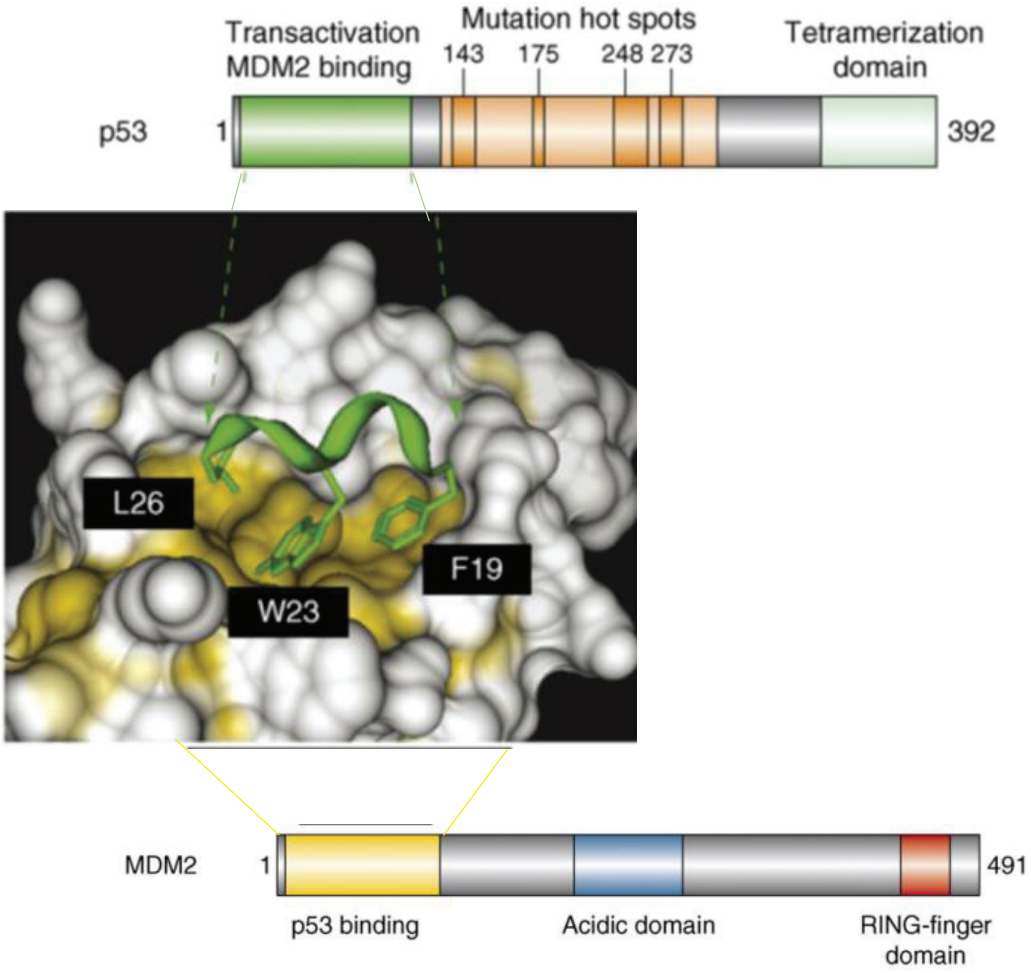

Figure 1.8. Structural representation of p53-MDM2 interaction [26].

The hydrophobic side of p53 alpha helix including Phe19, Trp23 and Leu 26 residues deeply insert into the hydrophobic cleft of MDM2 including Gly58, Glu68, Val75, or Cys77 residues as seen in figure 1.8. Thr18 residue of p53 alpha helix is important for its stability in MDM2-p53 interaction. MDM2 pocket is occurred by 26–108 aa and comprises two portions having close structural similarity folding up into a deep groove consisting of 14 hydrophobic and aromatic residues. A deep V-shaped cleft of MDM2 has several hydrophobic residues and is measured as 25 Å long, 10 Å deep and 10 Å width. The alpha helix of p53 is derived from 11 aa peptides, and the 2.5 turns of amphipathic alpha helix fit into MDM2 hydrophobic cleft by protruding Phe19, Trp23 and Leu26 residues of p53 into this cleft. Leu22 compacts against the surface of MDM2. A large proportion of molecular interactions is required for the strict association between p53 and MDM2 are Van der Walls contacts leading to buried surface area, although there are two intramolecular hydrogen bonds between them. Molecular analysis of MDM2 gene determined two types of mutation

blocking its interaction with p53 at residues D68 and C77 that are directly contact with the residues G58 and V75 of p53. These residues play role in structure of MDM2-p53 complex[27].

1.3.4. MDM2–Mediated Degradation of p53 in Proteasome

MDM2 is an E3 ligase that ubiquitinates p53 for its degradation on nuclear and cytoplasmic 26S proteasomes. For E3 ligase activity, MDM2 has RING finger domain (Zinc finger) on its evolutionary conserved carboxyl terminal. MDM2 catalyzes mono-ubiquitin tags onto lysine residues of COOH terminal on p53. MDM2-dependet-p53 degradation is started in nucleus by MDM2 binding to p300/CBP (CREB binding protein transcriptional coactivator proteins). MDM2 is capable of p53 mono-ubiquitination, whereas MDM2-P300/CBP catalyzes the poly-ubiquitination of p53 [9].

p53 activity depends on its cellular localization via nuclear import and export highly controlled. Nuclear import of p53 is provided by NLS (nuclear localization signal) motif in p53, whereas nuclear export of p53 is facilitated by two NES (nuclear export signal). Under stress, p53 is imported into nucleus via NLS to expose tetramerization, then binds to DNA for inducing the expression of related genes. p53 tetramerization is requisite for blocking nuclear export.

There are many protein affecting the localization of p53, the most significant one is MDM2. Except from the inhibition of p53 activity, MDM2 also regulates the nuclear-cytoplasmic shuttling of p53. MDM2 has NLS (nuclear localization signal) and NES (nuclear export signal) in its amino and carboxyl terminal which is necessary for nuclear export of MDM2. MDM2 is capable of shuttling in both directions on nuclear membrane. This function is important for decreasing p53 levels by binding to p53 in nucleus and export it from nucleus to cytoplasm for proteosomal degradation [28].

1.4. MDM2 Inhibitors

MDM2 is target for cancer therapy because of its important role in oncogenic process. The release of p53 from MDM2 stabilizes p53 to become activated in cell cycle arrest and apoptosis pathways. This is significant strategy for cancer therapy and prevention. There are many approaches to control of MDM2 for liberating p53 from it. These are the inhibition of

MDM2 expression , MDM2-P53 binding and MDM2 ligase activity [29]. To block MDM2 expression, antisense oligonucleotides have been designed. MDM2 expression is downregulated by oligonucleotides leading to p53 activation in cancer cells in vitro with tumor xenografts of nude mice [30]. When MDM2 inhibition is occurred, it was observed that cells with p53 protein becomes reactivated [31]. To block E3 ubiquitin ligase activity of MDM2 is other target for the activation of p53. Small molecule inhibitors have been recently identified for this purpose. Although they can activate p53 in apoptosis and cell cycle pathways, they are low potent and selective. The inhibition of MDM2-p53 complex is a challenging strategy because of targeting protein-protein binding with a small molecule. The small number of amino acid residues are enough for binding of p53 to MDM2. Phel9, Trp23 and Leu26 residues are necessary for p53 binding to MDM2, so small molecules are able to designed for mimicking this interaction [29].

1.4.1. MDM2 inhibitors in Clinical Trials

1.4.1.1. Cis-imidazolines

Nutlins are first potent small molecule MDM2 inhibitors that are based on 1,24,5-tetrasubstituted 4,5-cis-imidazoline structure. Nutlin-3 is the initial lead compound blocking MDM2-p53 interaction by inserting into p53 binding hydrophobic pocket with 90 nM IC_{50} value [32]. Nutlin-3 has been highly active in several cancer cells and showed anticancer activity in mouse xenograft model [33]. Nutlin-2 has two bromo-substituted phenyl rings interacting with Trp23 and Leu26 pockets of p53 and ethyl substituent on its third phenyl group occupying with Phe19 residue of p53. This mimics the three key hydrophobic residues of p53 peptide. Nutlin-3a (RG7112) have been firstly entered in clinical trials for patients with liposarcoma that having MDM2 amplification and wild-type p53 [34] [32]. In addition to this, RG7112 was investigated for leukemia cell types (AML, ALL and CML) [35].

1.4.1.2. Pyrrolidines

Idasanutlin (RG7388) having pyrrolidine structure demonstrates similar MDM2 inhibition activity with RG7112, but it is more potent and selective. In preclinical tests, idasanutlin shown anticancer effects on SJSA1 osterosarcoma xenografts models of nude

mice [36]. It induces p53 stabilization and p53-dependent pathways including apoptosis and cell cycle arrest in cancer cells with functional p53 [37].

1.4.1.3. Spirooxindoles

With based on the binding nutlins to hydrophobic pocket of MDM2, the oxindole ring mimics Trp23 residue in MDM2 binding domain of p53. It is important for p53 binding deeply into MDM2 hydrohobic cavity and NH group of Trp23 is interacted with carbonyl backbone of MDM2 via hydrogen bond. With this information, spiroxindole-derived inhibitors including indole group that could mimic Trp23 residue of p53 was designed. Spirooxindole having phenyl moiety which fit into the Phe19 binding cavity and isopropyl group mimicking Leu26 can dock into MDM2 pocket. RO-2468, RO-5353 and RO-8994 compounds are most potent spirooxindole derivatives with low nano molar IC_{50} values [34]. Spiroxindole analog MI-219 activates p53 by binding to MDM2 with 5 nM and Ki value. .MI-888 was more advanced compound with Ki=0.44 nM showed oral bioavailability in rats and provided tumor regression in two xenograft models. MI-888 and MI-77301 (SAR405838) can bound to MDM2 with 0.44 and 0.88 nM Ki values, respectively. They are more potent than nutlin-3 with Ki value of 43.6 nM. SAR405838 has been proceed into phase I clinical research , because of its high specificity to MDM2 [38]. Together with pimasertib that is MEK1 inhibitor, idasanutlin was tested in tumors. In xenograft melanoma models expressing wild-type p53, it was observed that the combination of SAR405838 and pimasertib have therapautic effect on tumor regression [39].

1.4.1.4. Isoquinolinones

The isoquilinone derivatives were developed as MDM2 inhibitor with using *in silico* screening. Among many compounds, NXN-7 was the most effective with 271 nM IC_{50} value, hovewer this compound was having low solubility and inducing apoptosis in healthy and cancer cells. CGM-097 and HDM201 compounds have been evaluated in phase 1 clinical researches. CGM-097 is most potent one in the series of isoquinolinone with 1.7 nM IC_{50} value. The X-ray crystallography results demonstrated that in CGM-097-Hdm2 complex, isopropoxy and metoxy groups are projecting to Leu26 residue, while carbonyl group of

dihydroisoquinolinone is forming H-bonds with carbonyl group of Phe55. 4-chlorophenyl group fit into Trp23 binding part in MDM2 hydrophobic pocket [32, 34].

1.4.1.5. Piperidinones and Piperidines

A tetrasubstituted piperidinone derivative AMG-8553 is most efficient and selective antagonists of MDM2-p53 interaction. In biochemical HTRF assay, it was indicated that this compound substantially blocked MDM2-p53 interaction with its IC_{50} value of 1.1 nM. In human SJSA-1 cells, this compound inhibited cell proliferation with 73 nM of IC_{50} value, However, its poor bioavailability was also shown in mouse models. The structure of this compound fits to the three important binding pocket of Leu26, Trp23 and Phe19of p53. By the optimization of AMG-8553, AMG-232 was produced. AMG-232 is another derivative of piperidinone family and has been currently investigated in phase I clinical trials [40]. AMG-232 importantly inhibits MDM2-p53 interaction in HTRF assay with 0.6 nM IC_{50} value. In SPR spectroscopy binding assay, it binds to MDM2 with Kd of 0.045 nM. In SJSA-1 cells having MDM2 amplification, this molecule decrease cell growth %50 at 9.1 nM by EdU assay. It also blocks the cell proliferation of HCT116 colorectal cancer cells having no MDM2 amplification with 10 nM IC_{50} in BrdU experiment. In efficacy studies, this molecule was exposed to SJSA-1 xenograft model with an ED_{50} of 9.1 mg/kg, and then tumor regression was observed [41].

1.4.1.6. Pyrimidinones

It was reported that pyrimidinone scaffolds have MDM2 inhibitor properties by molecular docking studies. In these studies, it was demonstrated that trifluoropyridine, trifluorothiophene and alkoxyphenyl rings imitates Phe19, Trp23 and Leu26 residues, individually. Piperidine and alkoxyphenyl moieties form Π-Π stacking bonding with Ty167 and His96 residues of MDM2 protein [32]. One of most potent compound from piperidines is MK8242 that has accomplished phase I trials in adults' leukemia and solid tumors. Although this compound is orally bioavailable, it has dose-limited property with hematological toxicity. Under high doses, it causes thrombocytopenia. In vitro studies, this

molecule is sensitive to cancer cells with wild type p53 with 0.07 IC_{50} μM value, however cancer cell lines with mutant p53 is resistant to MK8242 [42].

1.4.1.7. Peptides

Small peptides demonstrate 100-fold higher activity on MDM2 than p53, but they have low cell permeability problem. ALRN-6924 is a member of stapled peptides that was designed for disrupting p53 binding to MDM2/MDMX. According a study, ALRN-6924 is effective on ER positive cell lines including MCF7 and ZR-75-1, but it has no effect in no mutant p53 cell lines. Also, to enhance antitumor activity of ALRN-6924, it is combined with paclitaxel and erubilin. As a result of combination, ALRN-6924 is synergistic with these drugs [43].

CHAPTER 2

MATERIALS & METHODS

2.1. Cell Culture

2.1.1. Cell Thawing Out

The cryopreserved cells including HeLa, MCF7 and LNCaP were taken from -80 ^{o}C fridge, then warmed in 37 ^{o}C waterbath until thawing. After thawing of cells, cells were transferred into falcon tube including 3 mL medium. Falcon tubes were centrifuged at 800 rpm for 5 minutes. Next, supernatant was removed and pellet was dissolved with fresh medium. Finally, cells were cultured into T25 flask (SPL) including 5 mL medium, then incubated at 37 ^{o}C % 5 CO_2 culture environment.

2.1.2. Cell Lines

In this study, MCF7; HeLa and LNCaP cell lines as seen in table 1.1. were chosen to observe antiproliferative properties of compounds SM1-9. MCF7 and HeLa cells were obtained from the research laboratory of Assoc. Dr. Gülistan ÖZÇİVİCİ in Izmir Institute of Technology. LNCaP cell line was obtained from the research laboratory of Prof. Dr. Kemal Sami KORKMAZ in Ege University.

Table 2.1. The properties of MCF7, HeLa and LNCAP cell lines.

MCF7	HeLa	LNCaP
Human breast cancer cell line	Human uterus cancer cell line	Human prostate cancer cell line
Wild-type p53, MDM2 amplification	Wild-type p53, but not functional	Wild-type p53

MCF7 and HeLa cells were cultured in DMEM High Glucose medium (Biological Industries) containing 10% FBS, 1% penicillin and 1% L-glutamine; LNCaP cells were grown in RPMI-1640 medium (Biological Industries) containing 10% FBS, 1% penicillin and 1% L-glutamine in 5% CO_2 and 37 ^oC culture medium

2.1.3. Cell Culture Procedures

Before cell passaging, complete medium (DMEM or RPMI-1640) and trypsin (0.05%) were warmed in water bath at 37 ^oC. For passaging, firstly the present medium was removed from the flask, and flask surface was washed with new medium. Then, 1 mL trypsin was added onto MCF7 and HeLa cells at T25 flask for detaching cells from the surface of flask. Cells were waited in 37 ^oC and 5% CO_2 incubator for 3 minutes. LNCaP cells at T75 flask (SPL) were trypsinized for 2 minutes at incubator by adding 3 mL of trypsin. After incubation, 2 mL of complete DMEM was added onto flasks including MCF7 and HeLa cells and 6 mL of RPMI-1640 was added onto flask including LNCaP cells. For each cell lines, cells were collected from flasks and transferred into falcon tubes for each one. Next, centrifugation of cells was done at 800 rpm for 5 minutes. Supernatants were removed and pellets were dissolved with 1 mL of fresh medium. Finally, MCF7 and HeLa cells were transferred into new T25 flasks, whereas LNCaP cells were added into new T75 flasks. Cells were cultured in 37 ^oC and 5% CO_2 incubator until next passaging. MCF7 and HeLa cells were passaged 3 times a week, according to their growth rate and the condition of covering the flask surface as recommended in ATTC, whereas LNCaP cells were passaged twice a week.

2.2.4. Cell Counting

10 µL of cell suspension was gently mixed with 90 µL of tryphan blue dye by pipetting in 1.5 mL centrifuge tube (AXYGEN). Neubaer chamber was used for cell counting. Both sides of chamber were filled with approximately 10 µL of mixture. Then, live cells were counted under light microscope. After counting, the number of cells were determined by the formula as *the number of live cells x10 x* 10^4*(dilution factor)*.

2.2.5. Cell Freezing

Cells were dissolved into freezing medium including %50 DMEM or RPMI-1640, %40 FBS (fetal bovine serum), %10 DMSO (dimethyl sulfoxide). Then, cells were aliquoted in 1.5 mL cryotube (CORNING). Cells were stored at –80 ºC fridge for next usage.

2.2. MTT Cell Viability Assay

In this thesis, MTT (3- (4,5-dimethylthiazol-2-yl) -2,5-diphenyltetrazolium bromide) test was applied to examine the antiproliferative activity of tested compounds. In this context, the effects of compounds on the cells were analyzed after 48 hours of incubation. In first day, MCF7 and HeLa cells were seeded at 3000 cells per well into a 96-well plate (Thermofisher). LNCaP cells were seeded at 5000 cells per well and incubated at 37 ºC, 5% CO_2 culture medium for 24 hours. After 24 hours, all tested compounds (including the reference molecules such as pazopanib HCl and idasanutlin) were dissolved in DMSO to prepare seven different concentrations for each one. Cells treated with molecules were incubated at 37 ºC in 5% CO_2 culture medium for 48 hours. Later, 10 µL of MTT dye (5 mg/1 mL 1X PBS) was added to each well, and cells were incubated with the dye for 4 hours. At the end of this period, plate was centrifuged at 1800 rpm for 10 minutes. Then, supernatants in wells were removed. 100 µL of DMSO was added onto each well with multichannel micropipette to dissolve formazan and put onto shaker at 120 rpm for 15 minutes. Lastly, the absorbance of wells was measured with Thermofisher spectrophotometer at 560 nm. Cell viability was calculated by using following formula: %cell viability= sample absorbance*100/negative control absorbance. All molecules were tested three separate triplicate. The drawing of dose-response curves and GI_{50} calculations were performed by using Graphpad Prism 5 software.

2.3. Caspase 3/7 Activity Assay

According to the results of MTT experiment results, compounds SM8 and SM9 were chosen in order to investigate the induction of apoptosis due to their strong antiproliferative properties at low micro molar or nano molar concentrations. Because the activation of

caspases 3/7 are good sign for the induction of apoptosis, fluorometric caspase 3/7 activity test (Promega) was performed to observe the apoptotic effect of these molecules on LNCaP cells. Besides compounds SM8 and SM9, idasanutlin was used as positive control. In this experiment, LNCaP cells were inoculated into 96-well plates at 5000 cells per well and then incubated at 37 ^{o}C in 5% CO_2 for 24 hours. Next, cells were treated and incubated with one of the followings; 0.50, 2.95 and 12.00 μM concentrations of SM8, or 0.10, 0.22 and 4.00 μM concentrations of SM9, or 0.50,2.00 and 8.00 μM concentrations of idasanutlin for 24 hours at 37 ^{o}C in 5% CO_2. Then, 100 μL of Apo-ONE Caspase 3/7 reagent (Caspase Substrate Z-DEVD-R110 in Apo-ONE® Homogeneous Caspase-3/7 Buffer) was added to the wells. Plate was stirred at 200 rpm for 30 seconds on shaker. At the end of the 2 hours of incubation period, fluorescence intensities were measured by Biotek Synergy 1 instrument (Excitation: 428 nm and Emission: 520 nm). All experiments were done by three separate triplicates and statistical analysis were performed by One Way ANOVA in Graphpad Prism 5 software.

2.4. Annexin-V-FITC Apoptosis Assay

Annexin-V-FITC (Biovision K101-100) kit was used to observe the apoptotic effect of SM8, SM9 and idasanutlin in LNCaP cells. 500,000 LNCaP cells were seeded in each well of a 6-well plate, and incubated in culture medium at 37 ^{o}C 5% CO_2 for one day. At the end of one day, cells were treated one of the following with 0.50, 2.95 and 12 μM concentrations of compound SM8, and the 4.00, 0.22 and 0.10 μM concentrations of compound SM9; 8.00, .2.00 and 0.50 μM concentrations of idasanutlin for 24 hours. DMSO was added to the control cells at a final concentration of 1%. After 24 hours, the cells were collected by trypsinization from the wells of the 6-well plate and transferred to separate falcon tubes. It was then centrifuged at 800 rpm for 5 minutes. The pellet, whose supernatant was discarded after centrifugation, was dissolved in 1X PBS buffer solution. It was centrifuged again at 800 rpm for 5 minutes. After centrifugation, cells were dissolved in 200 μl of binding buffer. Then, 5 μL of Annexin-V-FITC dye and 5 μL of propidium iodide dye were added to each falcon tube in the dark. Finally, flow cytometry analysis was performed. All experiments were performed by two separate duplicates. Statistical analysis of flow cytometry results was done by One Way ANOVA in Graphpad Prism 5 software.

2.5. Cell Cycle Analysis by PI Staining

Cell cycle analysis method was used to examine the effects of compounds SM8 and SM9 cell cycle of LNCaP cell line. In the first day, the passaged cells were inoculated into the each well of 6-well plates at $4x10^5$ cells in 1980 µL of medium and incubated in culture medium at 37 ° C, 5% CO_2 for 24 hours. In the second day, compound SM9 was added to the wells at the final concentrations of 0.10, 0.22 and 4.00 µM in 20 µL of DMSO. 20 µL of DMSO with a final concentration of 1% was applied to control cells. For each molecule, 20 µl of 3 different concentrations were added to the wells. Plates were kept in the incubator for 24 hours. On the third day, the media collected from the wells were collected separately on the falcons. Then 500 µL of trypsin was applied for 1-2 minutes and cells were transferred from the wells to the falcons. The falcons were centrifuged at 800 rpm for 5 minutes. The supernatant was discarded, the pellets were dissolved in 5 mL of PBS and centrifuged again. The pellets, whose supernatants were removed, were dissolved in 1 mL of cold PBS. For each falcon, 4 mL of cold (-20 ºC) absolute ethanol was added dropwise while vortexing. Cells were incubated at -20 ºC for 24 hours. At the end of the 24-hour incubation time, the cells were centrifuged at 800 rpm speed and + 4 ºC for 5 minutes. After centrifugation, the supernatant was discarded and the pellets dissolved with 5 mL of PBS. It was centrifuged again. At last, 200 µL of PBS containing 0.01% Triton-X-100 is added on each pellet. Then samples were incubated at 37 ºC for 30 minutes with the incubation of 20 µL of RNAseA (1mg/mL). At the end of the incubation, 20 µL of propidium iodide (PI, 1mg / mL) was added onto samples. After the incubation of 15 minutes at room temperature, flow cytometry analysis was performed. Experiments were performed by two separate duplicates. Statistical analysis of flow cytometry results was done by One Way ANOVA in Graphpad Prism 5.

2.6. Fluorescence Polarization Assay

In this part of the thesis, fluorescence polarization assay was used to investigate possible MDM2 inhibitory properties of compounds SM1-9. Fluorescence polarization assay facilitated to observe the inhibition of MDM2-p53 interaction in the presence of these compounds and idasanutlin. Idasanutlin was used as positive control which demonstrates %100 inhibition in this study.

2.6.1. Fluorescence Polarization (FP) Buffer Preparation

All fluorescence polarization assays were performed in 100.00 mM phosphate buffer which has pH 7.5 prepared in 100 mL dH_2O. Additionally, 10 mg of γ-globulin and %0.02 sodium azide were added into this buffer solution and mixed by magnetic stirrer for 5 minutes.

2.6.2. Determination of FAM-PMDM6-F Probe Concentration

Firstly, 640 nM 5-FAM-PMDM6 (5-FAM-(β-A) -(β-A)-FM-Aib-pY-(6-Cl-DL-Trp)-E-Ac3c-LN-NH2) probe solution (fluorescent peptide strongly binds to MDM2 with K_d= 1 nM as reported in literature [44] was prepared from 1.0 mM 5-FAM-PMDM6 stock solution to determine the optimum working concentration of 5-FAM-PMDM6 probe. Then, starting from 640 nM concentration, twelve different 5-FAM-PMDM6 probe concentrations were prepared in black 96-well plate by two-fold dilution in 125 μL of FP buffer as duplicates. After 1 hour of incubation at room temperature, the fluorescence polarization values (mP) were measured with Biotek Synergy H1 instrument (Excitation: 485 nm, Emission: 560 nm). A graph of probe concentration dependent fluorescence polarization (mP) values was drawn by using Graphpad Prism 5 software. The minimum 5-FAM-PMDM6 probe concentration which showed stable mP value was chosen as working concentration for 5-FAM-PMDM6 probe.

2.6.3. Determination of MDM2 Concentration

Firstly, a solution of 400 nM MDM2 (1-118) protein was prepared from 50 μM MDM2 (1-118) protein stock solution in FP buffer. Starting from 400 nM concentration, twelve different MDM2 concentrations were prepared in black 96-well plate by two-fold dilution in 100 μL of FP buffer as duplicates. Then, 25 μL of 5-FAM-PMDM6 probe solution at 5 nM in FP buffer was added into each well in order to obtain 1 nM final concentration of 5-FAM-PMDM6 probe. Prepared MDM2-probe solutions were incubated at room temperature for 1 hour. After that, fluorescent polarization (mP) values of the prepared MDM2-probe solutions were measured with Biotek Synergy H1 instrument (Excitation: 485 nm, Emission: 560 nm).

A graph of MDM2 concentration dependent fluorescence polarization (mP) values was drawn by using Graphpad Prism 5 software. The minimum MDM2 protein concentration which showed stable and maximize mP value was chosen as working concentration for MDM2 protein in the presence of 1 nM 5-FAM-PMDM6 probe.

2.6.4. Determination of DMSO Concentration

At first, from 640 nm probe solution, 7.35 nM probe solution was prepared by dissolved in FP buffer. Then, 18.375 nM MDM2 solution was prepared from 400 nM MDM2 solution by dissolved in FP buffer. These solutions were mixed to obtain homogenous MDM2-probe solution which contains 1.47 nM probe and 14.7 nM MDM2. Starting with %32 DMSO concentration, twelve concentrations of DMSO were obtained in black 96- well plate by two-fold dilution in 125 µL MDM2-probe solution. The final concentrations of probe and MDM2 in each well was obtained 1 nM and 10 nM, respectively. Plate was incubated at room temperature for 1 hour. At the end of this period, fluorescence polarization (mP) values of MDM2-probe binding with twelve different DMSO concentration were measured with Biotek Synergy H1 instrument (Excitation: 485 nm, Emission: 560 nm). A graph of DMSO concentration dependent MDM2-probe binding were scratched by using Graphpad Prism 5 program. According to this graph, the effect of DMSO concentration on the stability of 5-FAM-PMDM6 peptide - MDM2 protein binding was determined.

2.6.5. Screening for MDM2 Inhibitors

In this part of fluorescence polarization assay, MDM2 inhibitory property of compounds SM1-9 was investigated. For this purpose, 8.33 nM probe solution and 41.66 nM MDM2 solution were prepared in FP buffer. Then, 60 µL of 8.33 nM probe solution and 60 µL of 41.66 nM MDM2 solution was added into black 96-well plate as 120 µL MDM2-probe solution per well. After that, 1000 µM solutions of compounds SM1-9 were prepared in DMSO. 5 uL of compound solution was added into wells to obtain 40 µM final concentration of testes compounds for each well. All compounds were tested in 2x2 wells. Plate was incubated at room temperature for 1 hour. After incubation, the fluorescence polarization values were measured with Biotek Synergy H1 instrument (Excitation: 485 nm, Emission: 560 nm).

Idasanutlin was used as positive control. MDM2-probe mixture with 4% DMSO was used as 0% inhibition reference. 4 nM probe solution in FP buffer with 4% DMSO was used as 100% inhibiton reference. Avarage and standard deviations were calculated. Statistical analysis was performed by using one-way ANOVA in Graphpad Prism 5 software.

CHAPTER 3

RESULTS & DISCUSSIONS

In this thesis, the antiproliferative properties of ezetimibe and synthesis intermediates that forms during ezetimibe synthesis on cancer cells were studied. Ezetimibe is lipid-lowering drug blocks dietetic cholesterol by inhibiting the Niemann-Pick C1-Like 1 (NPC1L1) that is cholesterol transport protein that play role in cholesterol absorption in the small intestine [45]. Until now, there is no study for investigating the anticancer effects of ezetimibe and intermediates formed during ezetimibe synthesis. Molecular docking studies demonstrate that compounds SM1-9 could inhibit MDM2 protein by binding to the same cavity that interacts witth p53. Thus, in this study, it was aimed at investigating antiproliferative effects of compounds SM1-9 on cancer cells along with the MDM2 inhibitory properties. With this purpose, MTT cell proliferation assay was performed for cytostatic or cytotoxic effects of compounds SM1-9. Selected two highly active compounds SM8 and SM9 were evaluated further for caspase 3/7 activity and Annexin V-FITC assays were applied to observe apoptotic induction. Lastly, fluorescence polarization assay was carried out to observe MDM2 inhibitory properties of these compounds. The results of these experiment were examined below.

3.1. MTT Cell Viability Assay

Cytotoxic agents are molecules that cause cell death, whereas cytostatic agents inhibit the cell proliferation without killing cells[46]. Cytotoxic or cytostatic profile of the compounds can easily be detected by using MTT assay. To investigate the antiproliferative effects of compounds SM1-SM9 in MCF7, HeLa and LNCaP cell lines, MTT cell viability assay was used. All of the compounds were tested up to 100 μM concentration as long as the lack of the solubility problem. The dose-response curves of compounds in all cell lines were demonstrated in Tables 3.1-3.5. For all of the tested compounds, GI_{50} values were calculated by using nonlinear regression analysis in Graphpad prism 5 software. These values were summarized in Table 3.6.

Pazopanib HCl, a multi-target tyrosine kinase inhibitor, was used as reference drug for comparison purpose[47]. In literature, pazopanib HCl is known as cytostatic agent rather than cytotoxic agent it can be a good guide to detect cytostatic compounds in cancer cells. Because pazopanib HCl is a well-known cytostatic properties of tested compound in literature, the numbers of cells in MTT assay should not be changed through the incubation time and there should not be growth inhibition more than %40-50 due to the inhibition of cell division.

As it is shown in Table 3.5, pazopanib HCl had minimum effect over cancer cell lines at low doses and it inhibits the growth of the cell lines up to %40-50 at higher doses. Even if the concentration of the drug increases, cell viability did not change after it reaches a plateau around %50 cell viability. After this point, pazopanib HCl dose response curve was used as reference to indicate the cytostatic properties of all tested novel compounds.

According to these results, tested compounds can be classified into three groups. In first group, compounds SM2, SM3, SM4 and SM6 exhibited cytotoxic property in all cell lines, whereas the second group consisting of compounds SM5, SM8 and SM9 showed cytostatic properties. Unlike these molecules, compound SM7 had no effect on all cell lines even if its maximum dose was applied (Table 3.4). Even though compound SM1 was listed in first group, it showed cytostatic effects only in MCF7 cell line with 29.95 μM GI_{50} value (Table 3.6), it did not have any cytostatic or cytotoxic activity on HeLa and LNCaP cell lines (Table 3.1).

There is not so much difference between the dose-response curves for compound SM2 in three cell lines (Table 3.1). However, nonlinear regression analysis demonstrated moderate cytotoxic activity for compound SM2 on MCF7 and HeLa cell lines with 47.58 μM and 51.43 μM values, besides stronger cytotoxic activity on LnCaP cells with 26.65 μM GI_{50} value (Table 3.6).

Table 3.1. Dose-dependent-cell viability curve of compounds SM1 and SM2 in MC7, HeLa and LNCaP cell lines.

	SM1	SM2
MCF7	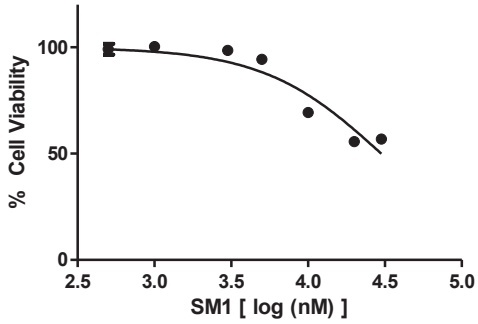	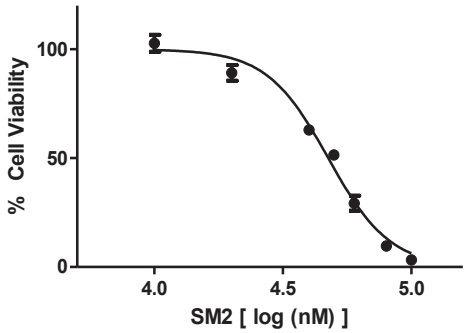
HeLa	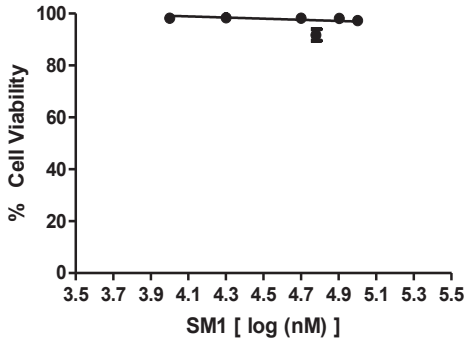	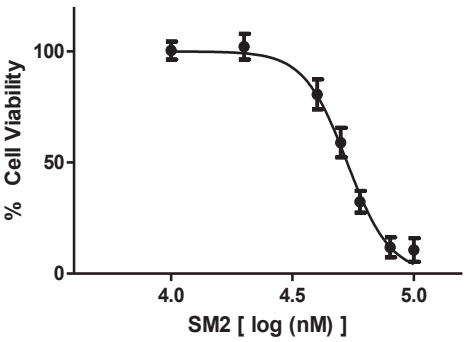
LNCaP	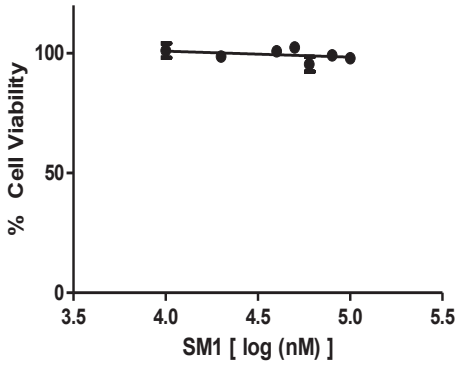	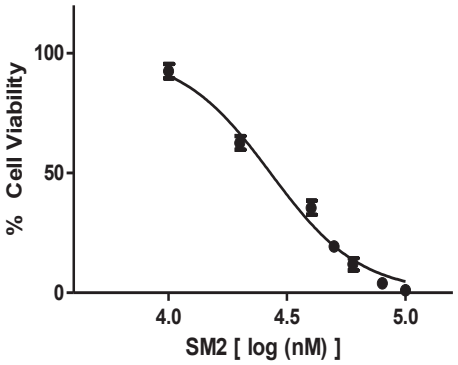

Table 3.2. Dose-dependent-cell viability curve of compounds SM3 and SM4 in MCF7, HeLa and LNCaP cell lines.

	SM3	SM4
MCF7	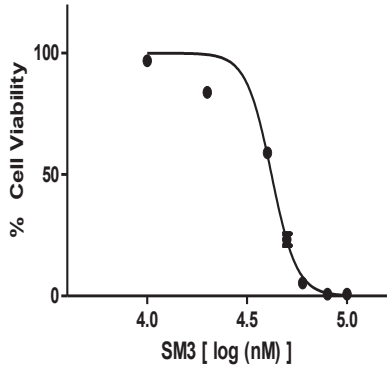	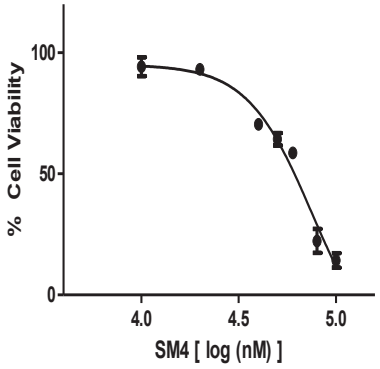
HeLa	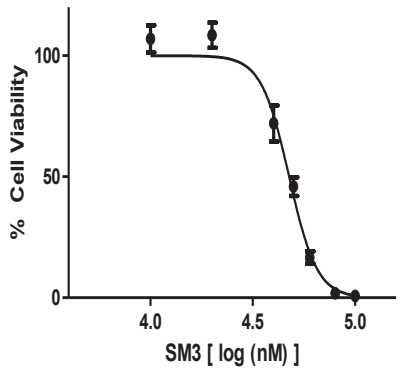	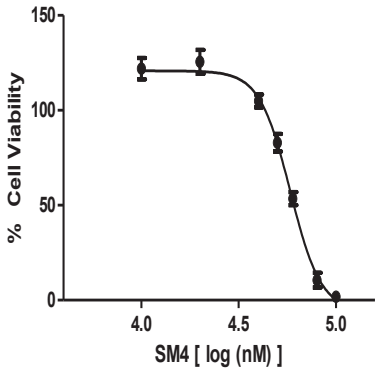
LNCaP	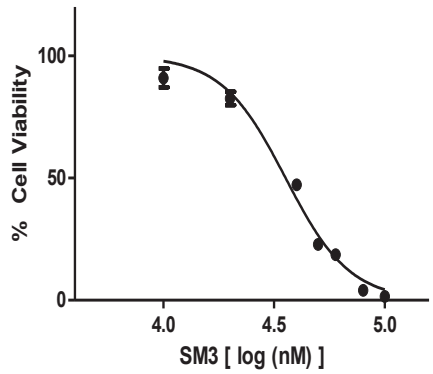	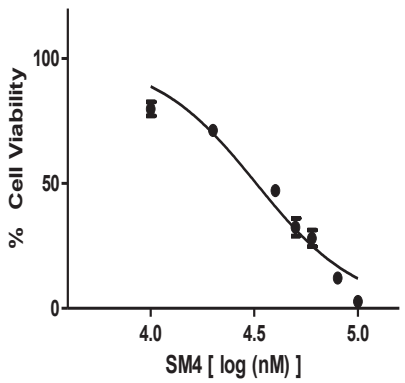

According to compound SM3 dose-response curve in Table 3.2, it has cytotoxic property on all cell lines. Additionally, compound SM3 had lower GI_{50} value in LNCaP cell line compared to other two cell lines, as seen in table 3.6. Compound SM4 had also cytotoxic property on all three cell lines in respect to the dose response curve in table 3.2. Similar to compounds SM2 and SM3, compound SM4 had higher cytotoxic effect on LNCaP cells with 33.19 μM GI_{50} value, whereas it showed moderate cytotoxicity on MCF7 and HeLa cell lines with 65.72 μM and 58.75 μM GI_{50} values (Table 3.6).

According the results in table 3.3, compound SM6 was placed in the first group because of its cytotoxic properties on all cell lines. Different from compounds listed in the first group, compound SM6 had closer GI_{50} values on all three cell lines (Table 3.6).

Compound SM5 was categorized in second group, because of its cytostatic effect on all three cell lines as shown in table 3.3. It demonstrated cytostatic properties on MCF7 and HeLa cell lines with 20.06 μM and 25.30 μM GI_{50} values respectively, while it had lower GI_{50} value that is 16.97 μM in LNCaP cell line (Table 3.6).

Compounds SM8 and SM9 were most active molecules among all tested compounds. These compounds indicated cytostatic activity on all cell lines at low doses. As seen in Table 3.4, compound SM8 led to %50 inhibition of cell grow at low GI_{50} values in all cell lines. As similar pattern with compounds in first group, SM8 had lower GI_{50} value which is 2.95 μM in LNCaP cells in contrast to MCF7 and HeLa cell lines whose GI50 values are 3.07 μM and 7.69 μM, respectively (Table 3.6). Compound SM9 had also high activity on MCF7, HeLa and LNCaP cells with 0.96 μM, 2.86 μM and 0.22 μM GI_{50} values, individually (Table 3.6). Compared to compound SM8, compound SM9 had lower GI_{50} values for each cell lines.

In literature, idasanutlin has cytotoxic effects on MCF7 and LNCaP cell lines with 2.0 μM GI_{50} value[48]. As seen in Table 3.6, it was found that idasanutlin demonstrated cytotoxic property on LNCaP cells with 0.798 μM GI_{50} value.

If compounds SM8 and SM9 is compared with pazopanib HCl, these compounds have cytostatic activity at lower concentrations than pazopanib HCl has. These compounds are able to decrease cell viability to %50 by inhibiting cell growth in all cell lines at low doses Thus, these compounds inhibit the proliferation of cancer cells. Because of these reasons, compounds SM8 and SM9 were chosen as two potent candidate molecules for investigating the apoptosis induction.

Table 3.3. Dose-dependent-cell viability curve of compounds SM5 and SM6 in MCF7, HeLa and LNCaP cell lines.

	SM5	SM6
MCF7	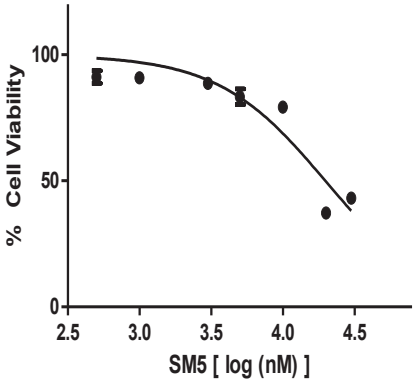	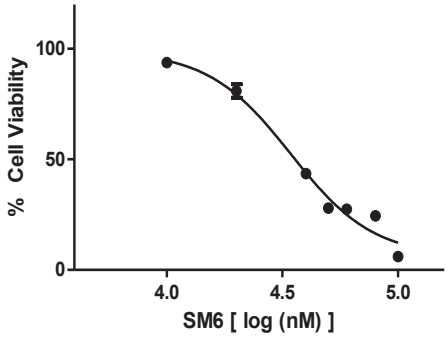
HeLa	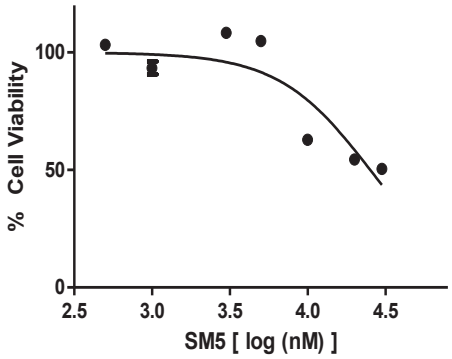	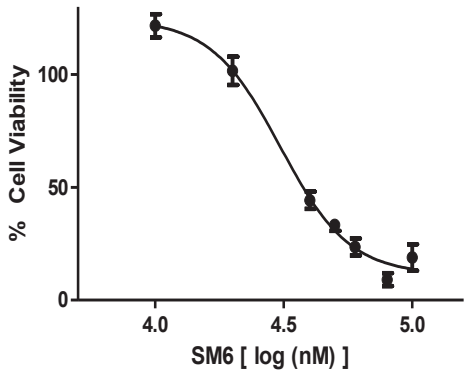
LNCaP	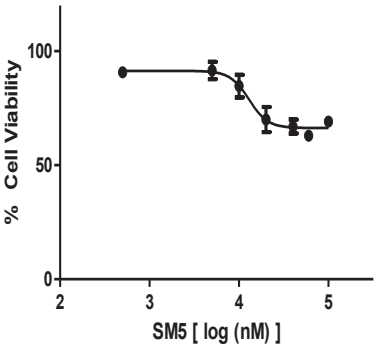	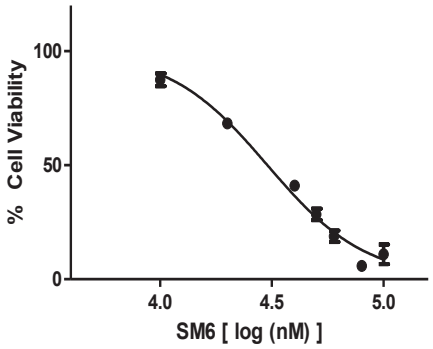

Table 3.4. Dose-dependent-cell viability curve of compounds SM7 and SM8 in MCF7, HeLa and LNCaP cell lines

	SM7	SM8
MCF7	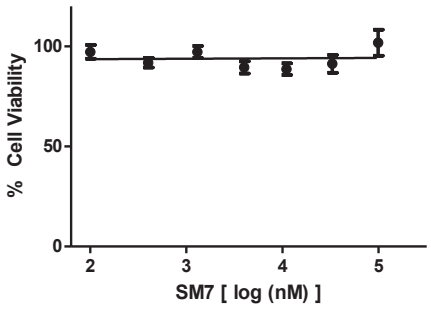	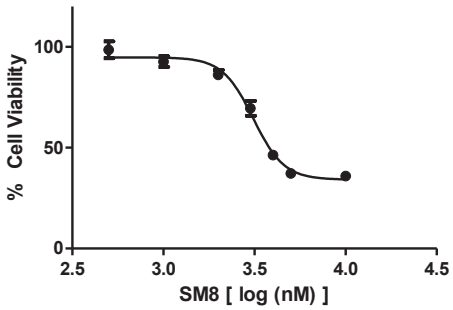
HeLa	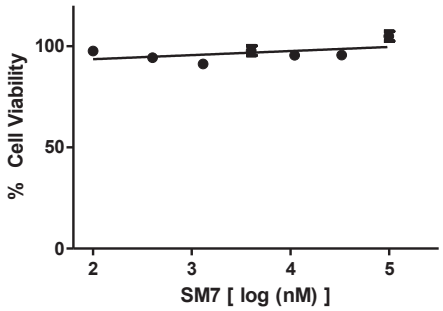	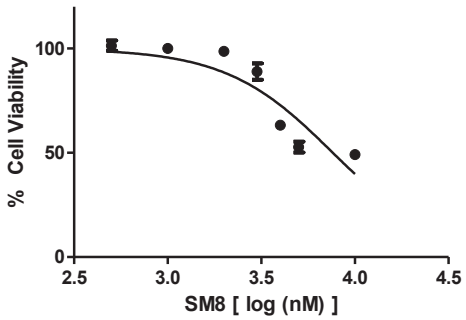
LNCaP	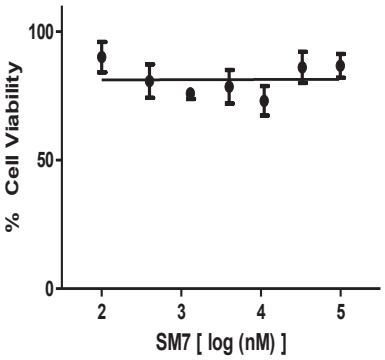	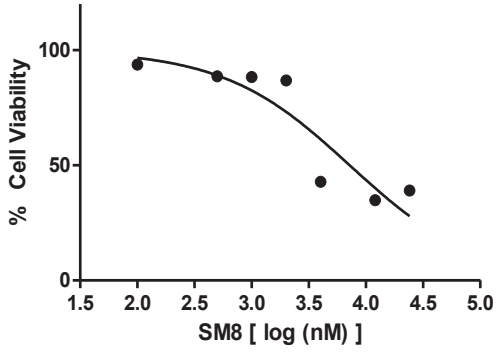

Table 3.5. Dose-dependent-cell viability curve of compounds SM9 and Pazopanib HCl in MCF7, HeLa and LNCaP cell lines

	SM9	Pazopanib HCl
MCF7	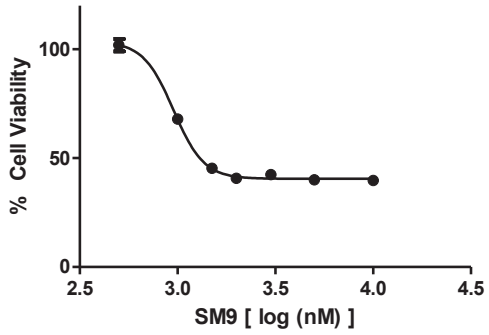	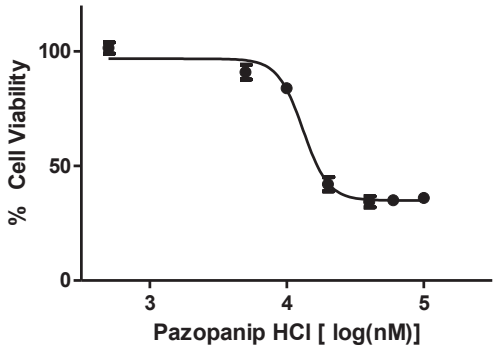
HeLa	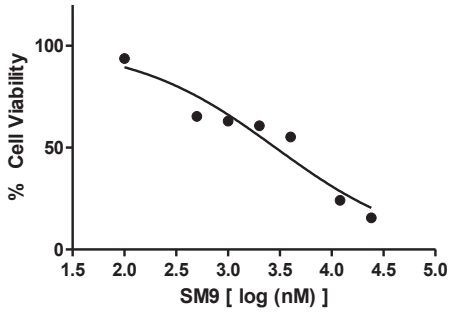	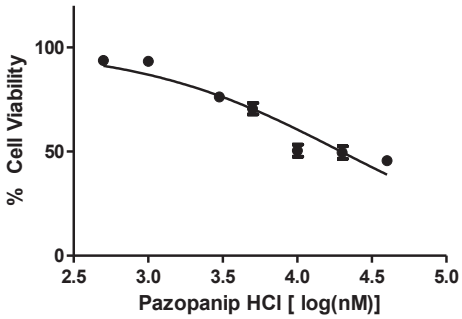
LNCaP	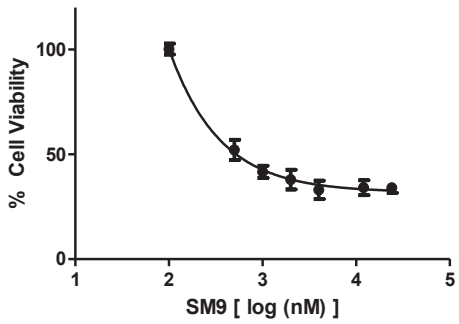	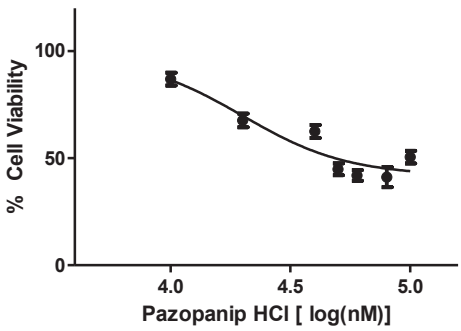

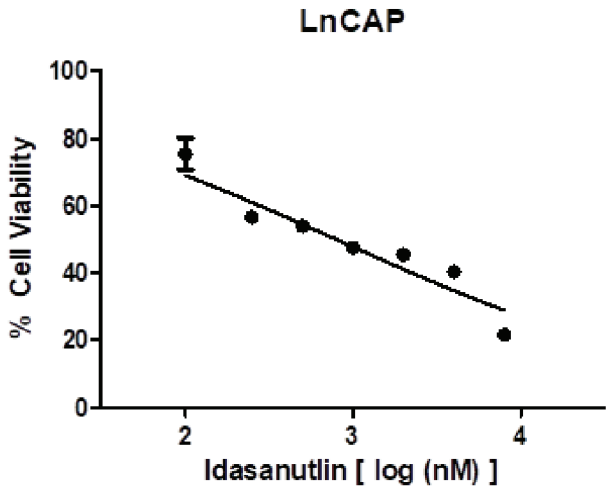

Figure 3.1. Dose-dependent-cell viability curve of idasanutlin in MCF7, HeLa and LNCAP cell lines.

Table 3.6. The GI_{50} values (μM) of compounds in MCF7, HeLa and LNCaP cell lines.

Compound	MCF7	HeLa	LNCaP
SM1	29.95 ± 3.37	-[a]	-[a]
SM2	47.58 ± 1.09	51.43 ± 7.11	26.65 ± 1.29
SM3	42.10 ± 1.76	47.85 ± 2.88	35.99 ± 1.95
SM4	65.72 ± 3.75	58.75 ± 7.3	33.19 ± 1.40
SM5	20.06 ± 1.76	25.30 ± 1.85	16,97±1,89
SM6	33.71 ± 1.62	28.98 ± 1.72	30.23 ± 2.12
SM7	-[a]	-[a]	-[a]
SM8	3.07±0.27	7.69 ± 1.09	2.95 ± 0.10
SM9	0.96±0.03	2.86 ± 0.39	0.22 ± 0.6
Pazopanip.HCl	13.03±0.92	19.79 ± 3.15	18.36 ± 4.28
İdasanutlin			0.798±0.25

[a]Cell viability is over 50% at all tested concentrations (or no cytotoxicity)

3.2. Fluorometric Caspase 3/7 Activity Assay

MTT results indicated that compounds SM8 and SM9 are two promising drug candidate by showing cytostatic properties in all tested cell lines at low micromolar and nanomolar concentrations. Because of that, they were chosen for induction of apoptosis. LNCaP cell line were selected for two reasons. The first, it expresses wild-type p53 protein and in the case of MDM2 inhibition, the induction of apoptosis can be expected. The second, compounds SM8 and SM9 showed highest activity on LNCaP cell line compare to other cell lines.

The activation of caspases 3 and 7 are good sign for the induction of apoptosis. In this assay, the amount of activated caspases 3 and 7 were measured in LNCaP cancer cells treated with compounds SM8 and SM9. DMSO-treated LNCaP cells were used as negative control and idasanutlin was used as reference drug for comparison purpose. The fluorescence intensity in figure 3.1 illustrates the activity of caspases 3/7 in LNCaP cells treated with idasanutlin, compounds SM8 and SM9 for 24 hours.

All of the compounds were tested at their GI_{50} values and two additional doses. As shown in Figure 3.2, there is a slight increase in the amount of activated caspases 3/7 in the presence of 0.50 μM and 2.00 μM concentrations of idasanutlin. Only statistically significant and dramatic increment of caspases 3/7 was observed in LNCaP cells treated with 8.00 μM of idasanutlin. The caspases 3/7 activity slightly increased in LNCaP cells under the treatment with 0.50 μM, 2.95 μM and 12.00 μM doses of compound SM8 as comparing to negative control. However, there was not significant increment in high dose of compound SM8, as in that of idasanutlin. Even if 12.00 μM concentration of compound SM8 did not dramatically increase caspases activity, in contrast to 8 μM concentration of idasanutlin. As seen in figure 3.2, compound SM9 induced caspases 3/7 activity in LNCaP cells at 0.10 μM, 0,22 μM and 4.00 μM concentrations. Both compounds SM8 and SM9 increased caspases 3/7 activity without depending on their doses, whereas idasanutlin led to increase the activation of caspases 3/7 in dose-dependent manner.

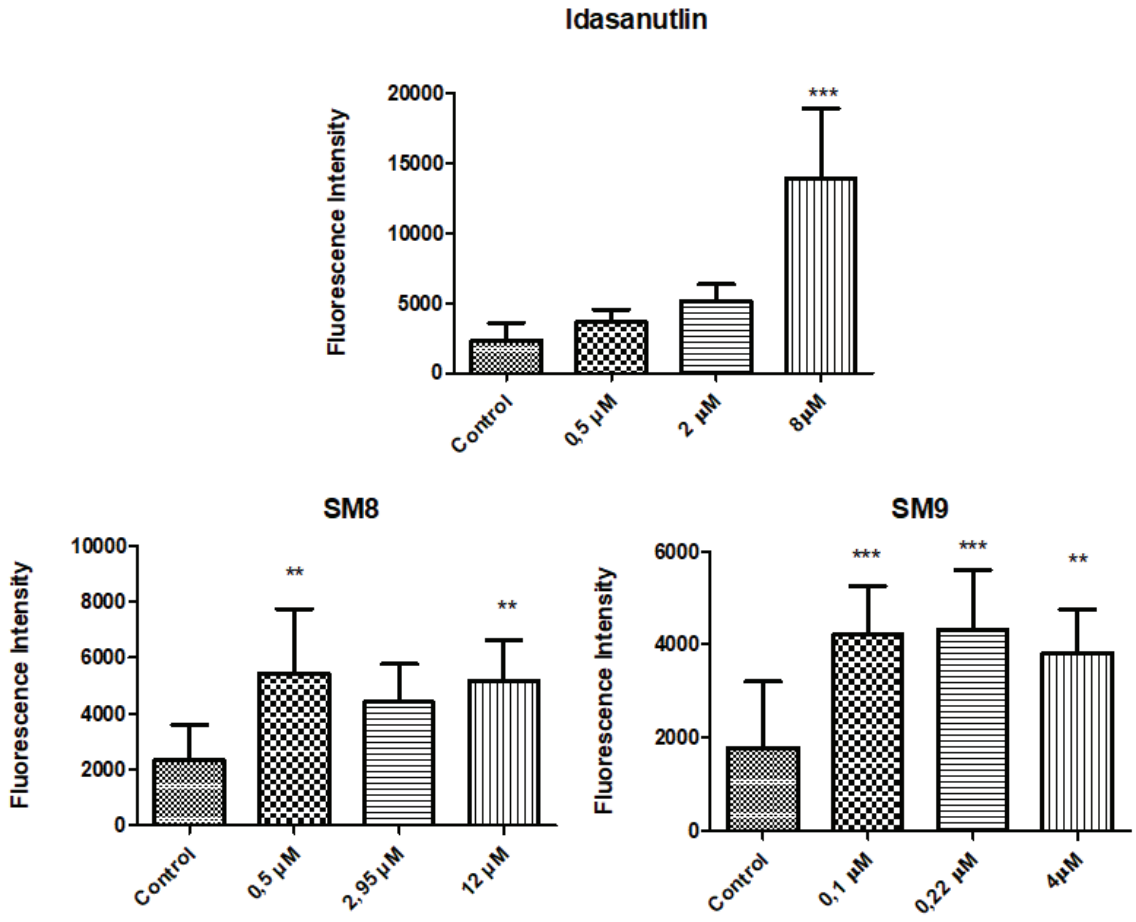

Figure 3.2. Fluorescence intensity demonstrate caspases 3/7 activity in LNCaP cells under the treatment of compounds SM8, SM9 and idasanutlin. (One-way ANOVA analysis by Graphpad Prism 5. *** $p \leq 0.001$, ** $p \leq 0.01$).

3.3. Annexin V-FITC Apoptosis Assay

In this part of study, the apoptotic effects of compound SM8 and SM9 were studied by using Annexin-V FITC assay. In normal conditions, cells have asymmetric distribution of phospholipid in two side of cellular membrane. Phosphatidylserine (PS) is found on the cytoplasmic side of cellular membrane. In early apoptosis events, membrane asymmetry is quickly lost. This causes the translocation of PS to the extracellular surface of membrane which provides recognition and removal of death cells via phagocytosis. FITC labeled Annexin V has high affinity for phosphatidylserine (PS) in the existence of Ca^{2+}. By this way, apoptotic cells are detected. Propidium iodide (PI) is impermeable DNA dye added into cell suspension to discriminate early apoptotic cells from late apoptotic and necrotic cells which lost membrane integrity.

İdasanutlin was used as reference drug at the same doses used in Caspase 3/7 activity assay. In literature, idsanutlin strongly binds to MDM2 protein resulting in the induction of $p21^{WAF1/CIP1}$ by the reactivation of p53. Idasanutlin affect the induction of cell cycle arrest by the elevating $p21^{WAF1/CIP1}$ resulting in the elevation of BAK and BAX proteins in LNCaP cells. In this process, BAK and BAX causes the cleavage of PARP that is marker for apoptosis [49].

According to the results of MTT assay, compound SM8 inhibited the growth of LNCaP cells %50 at 2.95 μM concentration. Thus, 0.50 μM, 2.95 μM and 12.00 μM concentrations were chosen to study the apoptotic effect of this compound in LNCaP cell line. Flow cytometry analysis in Figure 3.3 and Figure 3.4 showed that compound SM8 had no effect on apoptotic induction in LNCaP cells as expected. As seen in figure 3.2, compound SM8 did not induce early apoptosis (Q4) in LNCaP cells at 0.5 μM, 2.95 μM and 12 μM concentrations. However, it moderately affected late apoptotis (Q2). Additionally, this compound led to necrosis in small percentage of LNCaP cells.

As similar with compound SM8, compound SM9 merely induced late apoptosis in LNCaP cells at 0.1 μM, 0.22 μM and 4 μM concentrations, whereas it had no effect on early apoptosis in LNCaP cells (Figure 3.3 and Figure 3.4). This compound also led to necrosis in small portion of cells. Additionally, these results are correlated with the caspase 3/7 assay results.

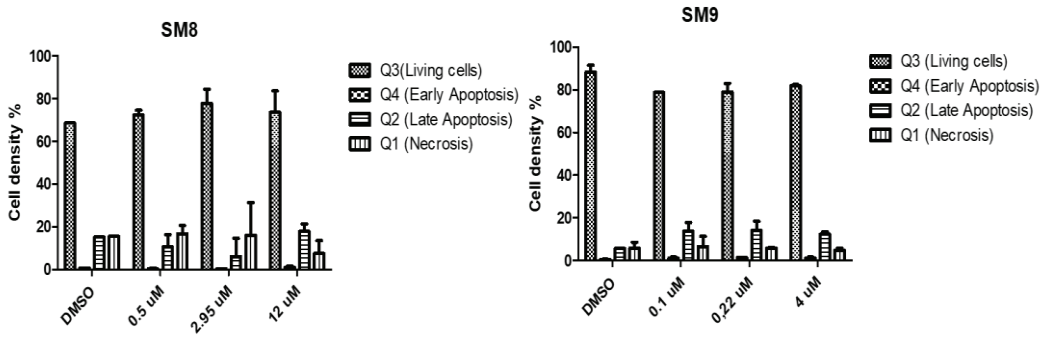

Figure 3.3. The bar graph for the apoptotic effects of compounds SM8 and SM9 on LNCaP cells at different concentrations. (One-way ANOVA analysis by Graphpad Prism 5. *** $p \leq 0.001$, ** $p \leq 0.01$).

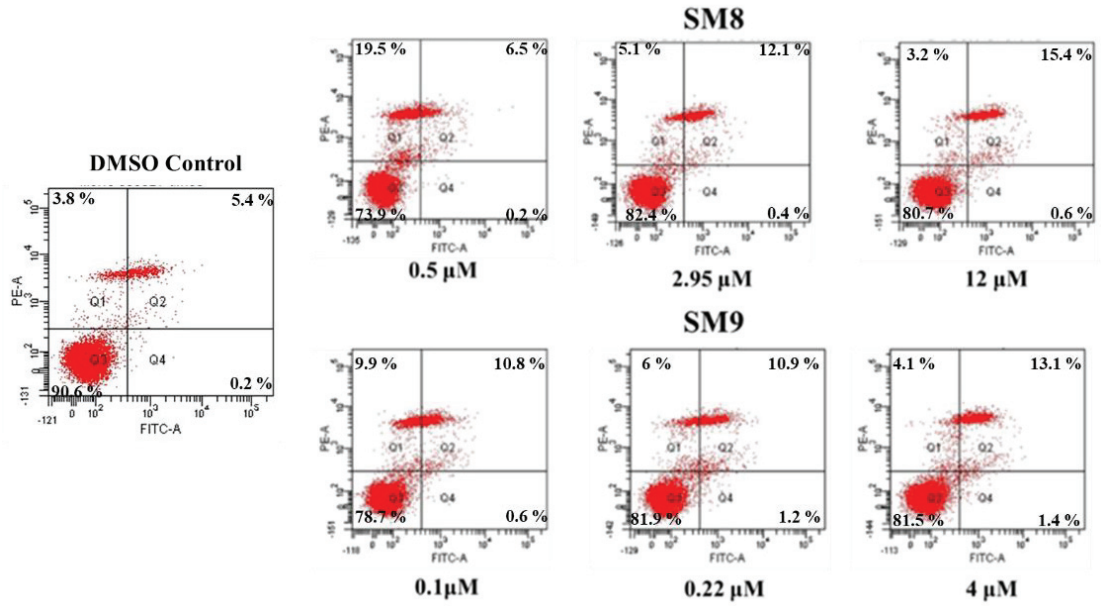

Figure 3.4. Histograms for the apoptotic effects of the compounds SM8 and SM9 on LNCaP cells analyzed by flow cytometry. Q3: Live cells, Q4: Early apoptosis, Q2: Late apoptosis and Q1: Necrosis.

3.5. Cell Cycle Analysis by PI Staining

The cytostatic property of compound SM9 was studied in LNCaP cells, by propidium iodide staining in this party of thesis. LNCaP cell line was used to analyze cell cycle profile, because of its having wild type p53 higher activity of compound SM9 in this cell line. Cell cycle analysis of LNCaP cells under the treatment of compound SM9 was performed by flow cytometry. Cell cycle analysis is common procedure to use flow cytometry for measuring DNA contents of cells. In this procedure, propidium iodide that is fluorescent dye can bind to DNA which is incubated with a cell suspension of fixed or permeabilized cells. PI can bind to DNA stoichometrically, meaning that fluorescent intensity of dye is directly proportional to DNA amount. By flow cytometry, the percentage of the population in G0/G1, S, and G2/M phases can be determined.

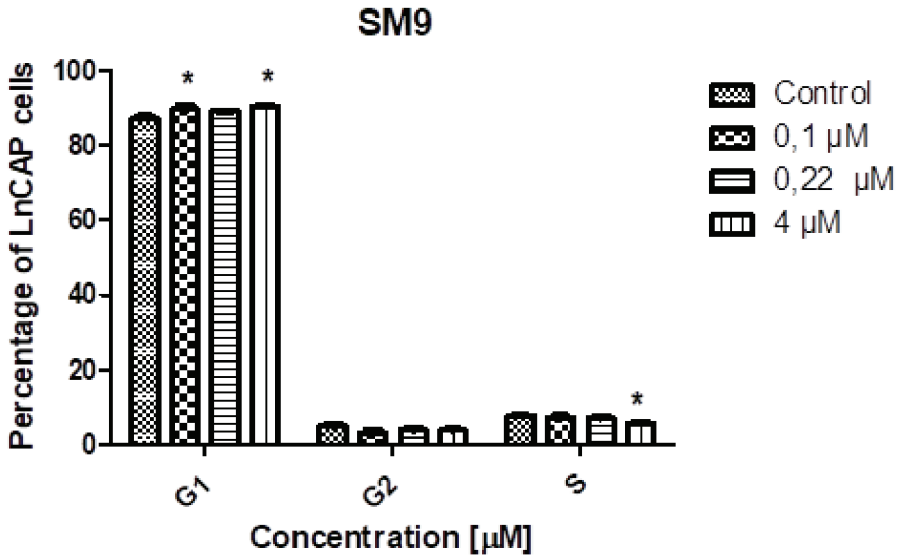

Figure 3.5. The bar graph of the effects of compound SM9 on cell cycle phases of LNCaP cells at 24 h. (One-way ANOVA analysis by Graphpad Prism 5. * $p \leq 0.05$).

According to results of this experiment in figure 3.5, compound SM9 demonstrated effect on G1 phase of LNCaP cells. Because the higher percentage of cells were found in G1 phase when they treated with 4.00, 0. 22 and 0.10 µM concentrations of compound SM9 for one day. At 4.00 µM and 0.10 µM concentrations of compound SM9, statistically significant increase with low standard deviation was observed at G1 phase of LNCaP cells comparing to control LNCaP cells (treated with DMSO). At G2 phase of LNCaP cells, there are no significant differences between control cells and cells treated with compound SM9. 4.00 µM concentration of compound SM9 resulted in slight decrease in the percentage of LNCaP cells

at S phase. This result is statistically significant with low standard deviation ($p \leq 0.05$). These results showed that compound SM9 has cytostatic activity on LNCaP cells.

3.4 Fluorescence Polarization (FP) Assay

Fluorescence polarization assay is used to detect protein-protein interaction. This method is performed to measure molecular interactions. The binding and dissociation between two molecules are measured by the rate of molecule rotation. If one of two molecules is small and fluorescently labeled, this molecule rotates rapidly in the solution. When it binds to larger molecules such as protein, its rotation becomes slower. Free molecule is excited by polarized light, but emitted light from this molecule remains depolarized, so freely rotating fluorescent molecule gives low polarization signal. When this fluorescent molecule binds to larger molecules such as protein, its rotation becomes slower. Upon excitation of this complex by polarized light, much of emitted light becomes polarized, because of slow rotation of the complex. As a result of this, the fluorescence polarization (FP) signal increases.

In this assay, FAM-PMDM6-F probe is fluorescently labeled p53 peptide which is bound to MDM2 protein. It was observed that FP signal increased when these molecules bind to each other. FP signal were monitored at excitation 428 nm and emission 560 nm.

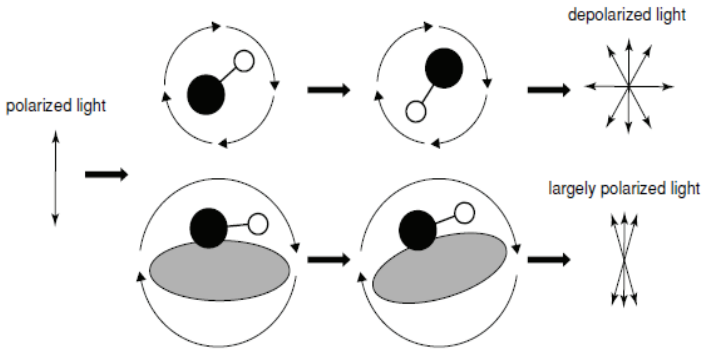

Figure 3.6. The schematic explanation of FP assay theory. The rapidly rotating small flurophore gives a low FP signal. When its binding to large molecule such as protein, its rotation will slow down, resulting in an increased FP signal (Moerke, 2009).

3.4.1. Determination of FAM-PMDM6-F Probe Concentration

FAM-PMDM6-F probe (p53 mimicking peptide) gives fluorescence polarization in excitation 428 nm and emission 560 nm. Starting with 640 nM, 12 different concentrations of probe were prepared by two-fold dilutions. Stability of the FP values depends on the probe concentration. Thus, it would be expected that high probe concentration gives low polarization signal. In this part of the study, determination of the smallest 5-FAM-PMDM6-F probe concentration that gave stable FP reading was aimed.

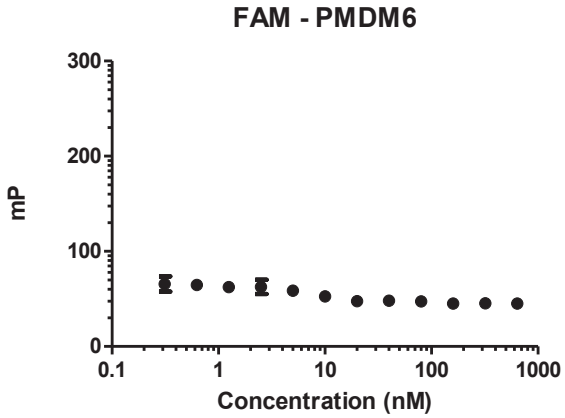

Figure 3.7. The fluorescence polarization (mP) values of FAM-PMDM6-F probe at different concentrations. Ex: 428 and Em: 520.

According to figure 3.7, all probe concentration demonstrated stable polarization signal, so all concentrations were seemed suitable for working. In literature, working concentration of probe for MDM2 binding, 1 nM probe concentration was chosen for determining MDM2 concentration [44].

3.4.2. Determination of MDM2 Concentration

Starting with 320 nM, 12 different concentrations of MDM2 were prepared by two-fold dilutions to detect optimum concentration of MDM2 which gives stable and maximized FP signal with 1 nM probe. It was hypothesized that the polarization values MDM2-probe complex would increase by increasing the MDM2 concentrations. However, at 10 concentrations of MDM2, the FP values of this complex had stable FP values about 150 mP,

except from 320 nM and 160 nM concentrations. Before 100 nM concentration, FP values became stable in figure 3.8. Because FP values were stable in wide-range of MDM2 concentrations. 10 nM MDM2 concentration was preferred according to literature[44].

One important point is the obtained MDM2 concentration dependent FP results have some deviations from the expected. As mentioned before the mP readings should be increasing concentrations of MDM2. High mP readings even at less than 1 nM MDM2 protein in the presence of 1 nM probe imply some non-specific binding of the peptide to the protein. It might be possible that MDM2 might be some structural changes due to the storing at -20 ^{o}C during COVID-19 pandemic period.

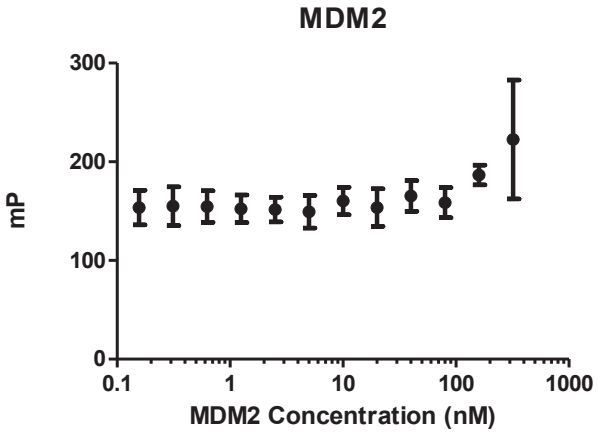

Figure 3.8. The fluorescence polarization (mP) values of MDM2/FAM-PMDM6-F probe binding at different MDM2 concentrations with 1 nM concentration of FAM-PMDM6-F probe. Ex: 428 and Em: 520.

3.4.3. Determination of DMSO Concentration

The effects of DMSO concentration on MDM2- FAM-PMDM6-F probe binding were investigated by using 12 different DMSO concentration (%)which was obtained by two-fold dilutions. The FP signal of MDM2-FAM probe with different DMSO concentrations was measured at excitation 428 nm and emission 560 nm.

It was expected that DMSO concentration affects the MDM2-FAM probe binding. According to results of experiments, DMSO did not demonstrate effect on MDM2-p53 complex depending on its concentration. This result was resulted from MDM2 protein that was used. Because of this, %4 DMSO concentration was determined to work in later experiments.

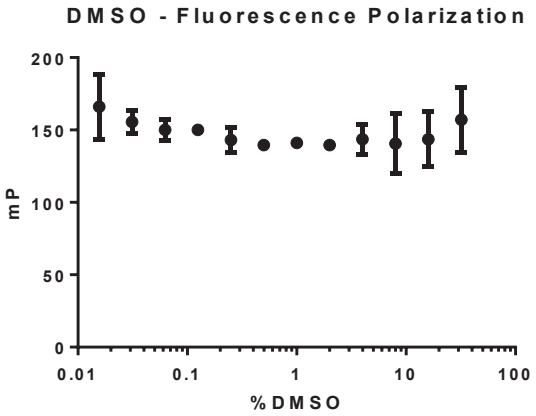

Figure 3.9. The fluorescence polarization (mP) values of MDM2/FAM-PMDM6-F probe binding with 1 nM probe and 10 nM MDM2 concentrations at different concentration of DMSO (%). Ex: 428 and Em: 520.

3.4.4. Inhibition of MDM2-prob binding in the presence of idasanutlin

Idasanutlin is an MDM2 inhibitor, which was used as positive control in this assay. With using idasanutlin, the inhibition of MDM2- FAM probe complex was demonstrated. 2.00 μM idasanutlin was added into solutions containing different concentrations of MDM2 and 1 nM probe.

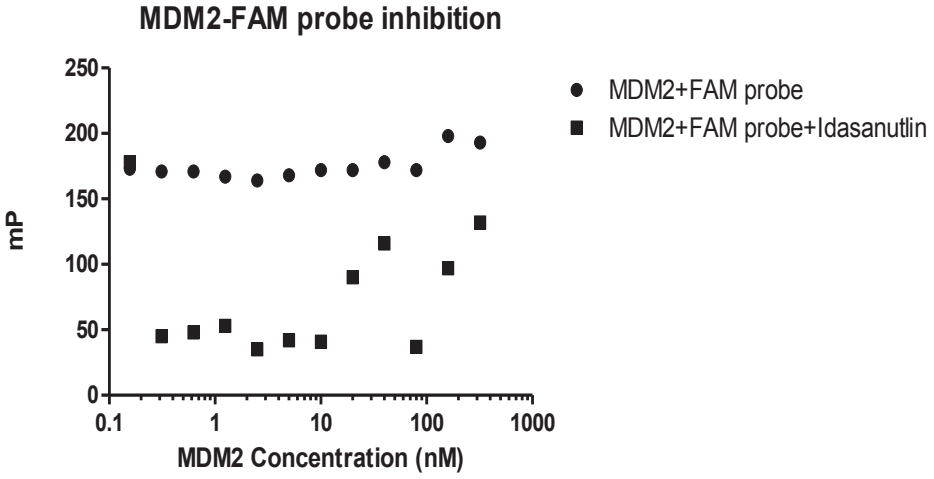

Figure 3.10. The inhibition of MDM2-probe binding in the presence of idasanutlin at 2.00 μM. Ex: 428 and Em: 520.

Figure 3.10 demonstrates the FP values of MDM2-probe (FAM-PMDM6-F) without and with idasanutlin. Before adding idasanutlin, the FP values of MDM2-prob complex at twelve different MDM2 concentrations which were studied in previous step, FP values of this complex were higher. After idasanutlin treatment, the FP values of this complex dramatically decreased, except from 320, 160, 80, 40 and 20 nM concentrations of MDM2 protein. Below 10nM MDM2 concentration, low and stable FP values were obtained indicating the disruption of MDM2-probe complex. Thus, 10 nm MDM2 and 1 nM probe was approved as suitable working concentration for drug screening experiment.

After these experiments, drug screening studies were performed. However, MDM2-probe complex could not be inhibited when it was treated with any of the tested compounds and idasanutlin because of its FP value had been still high. In this point, it was suspected that MDM2 protein was not stable in FP buffer and decomposes during storage at -20 ^{o}C. Hence a new stock of MDM2 protein was used for further experiments.

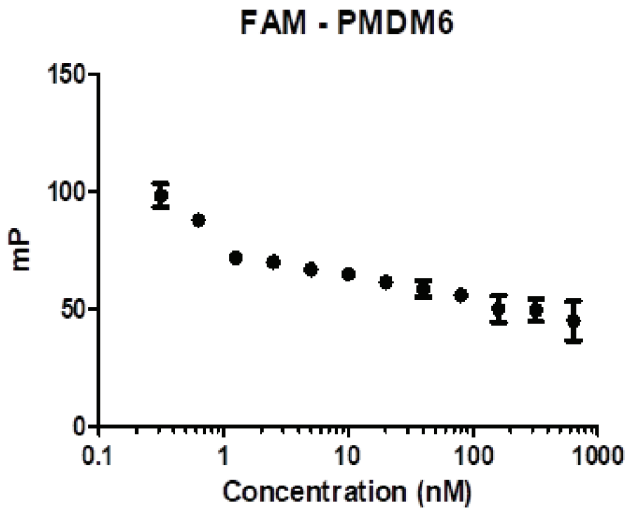

Figure 3.11. The fluorescence polarization (mP) values of FAM-PMDM6-F probe at different concentrations. Ex: 428 and Em: 520. Probe dissolved in DMSO.

By using new stock of MDM2 protein, similar studies were performed to determine protein and probe concentrations. As shown in figure 3.11 and 3.12, it was seen that FP values of MDM2-probe complex slightly decreased., however FP values of probe concentrations remained stable, after 1 nM concentrations. Although FP values in different concentrations of probe were same as previous experiment, we observed that lower fluorescence intensity at each concentration, in figure 3.11.

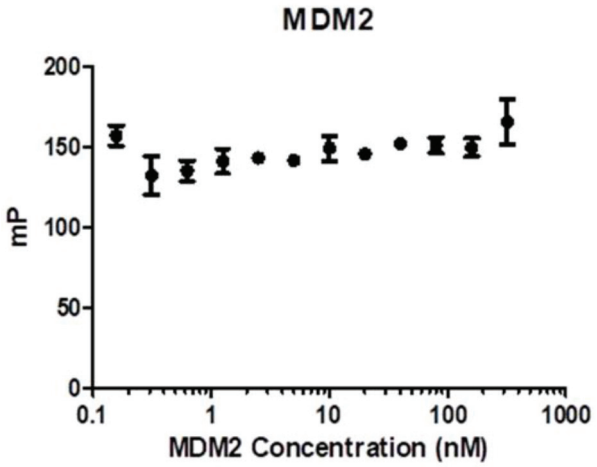

Figure 3.12. The fluorescence polarization (mP) values of MDM2/ FAM-PMDM6-F probe binding at different MDM2 concentrations with 1 nM FAM-PMDM6-F probe concentrations. Ex: 428 and Em: 520.

In figure 3.12, mP values of MDM2-probe complex had still been unchanged depending on MDM2 concentration. Unchanged FP values of this complex at different MDM2 concentrations was resulted from nonspecific binding of probe to MDM2 at low concentrations. Even if treatments with 1000 μM idasanutlin, FP value of MDM2-probe complex could not be reduced. It was thought that Mdm2 protein undergoes conformational changes during storage at -20 ^{o}C.

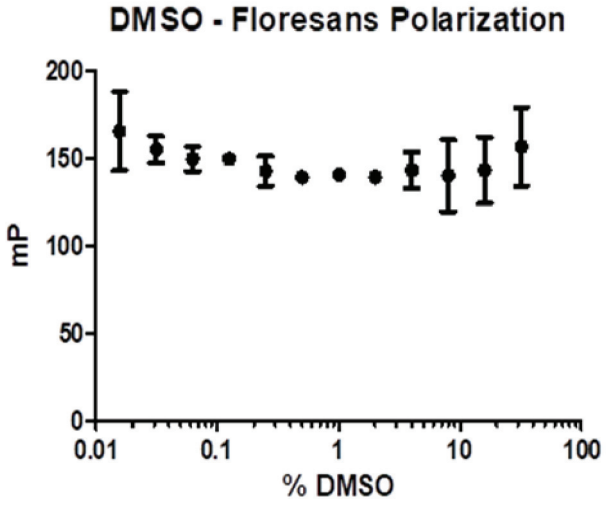

Figure 3.13. The fluorescence polarization (mP) values of MDM2/ FAM-PMDM6-F probe binding with 1nM probe and 10 nM MDM2 concentrations at different concentration of DMSO %. Ex: 428 and Em: 528.

The effect of DMSO on MDM2-probe complex at different concentration was investigated. Same results with previous DMSO experiments were obtained as seen in figure 3.13., and it was continued to work with %4 DMSO. Similar experiments were performed by new stock of MMD2 protein, In the presence of idasanutlin, FP value of MDM2-probe complex was decreased from 110 to 85 mP. Same experiments gave reproducible results, so it was determined to use 4 nM probe and 20 nM MDM2 protein for drug screening studies.

3.4.5. Screening for MDM2 inhibitors

Drug screening experiments were done for examining the inhibitory effects of compounds on MDM2-probe interaction. For this purpose, 4 nM probe and 20 nM MDM2 protein solution was incubated with 40 µM concentrations of compounds SM1-9 (except SM7) and idasanutlin for 1 hour. When FP values were monitored, graph in figure 3.14 was obtained.

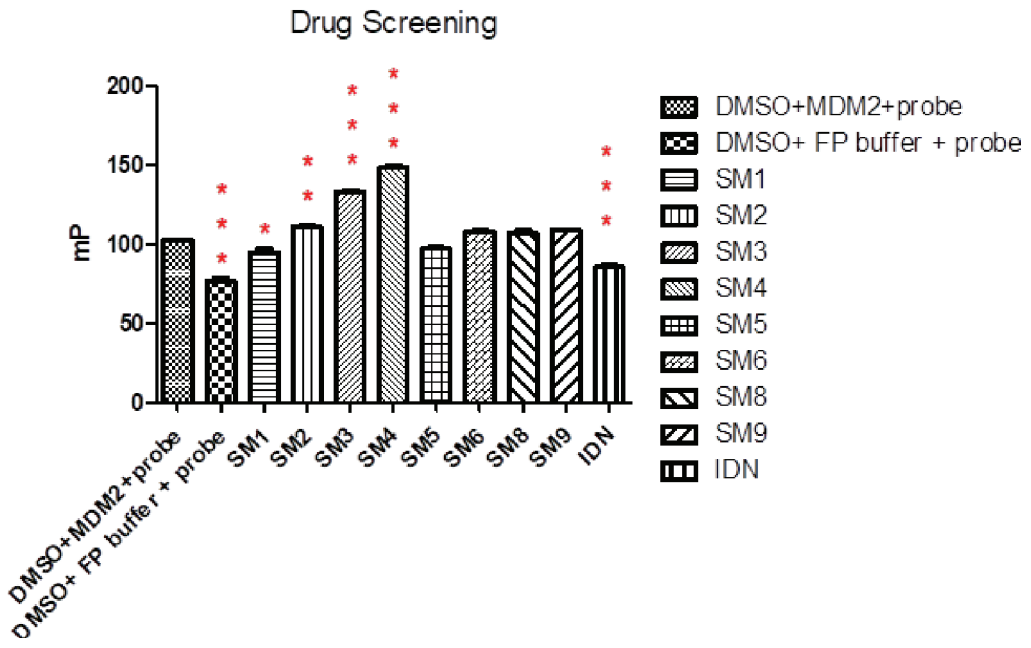

Figure 3.14. The fluorescence polarization (mP) values of MDM2/FAM-PMDM6-F probe binding with 4nM probe and 20 nM MDM2 concentrations under the treatment of compound SM1-9 (excepted from compound SM7) and idasanutlin at 40 µM concentration. Ex: 428 and Em: 520. (One-way ANOVA analysis by Graphpad Prism 5. *** $p \leq 0.001$, ** $p \leq 0.01$).

In here, DMSO-probe demonstrates the reference points for %100 inhibition due to the lack of MDM2 protein, whereas DMSO-MDM2-probe indicates %0 inhibition. The FP value of DMSO-MDM2-probe solution was around 102,12 mP which is FP value of MDM2-probe interaction. DMSO- FP buffer- probe solution was around 77,33 mP that is free probe FP value.

As seen in figure 3.14, the FP value of this complex in the presence of idasanutlin that is positive control was closer to the FP value of DMSO-probe. This demonstrates that idasanutlin can inhibit MDM2-probe interaction as regarded in the literature. This result is statistically significant because p value is smaller than 0.001.

The FP value of sample treated with compound SM1 was between the FP values of DMSO-MDM2-probe and DMSO-probe readings. This shows that it has weak inhibition activity on MDM2-probe interaction. In the existence of compound SM5, the FP value of this complex was smaller than the FP value of DMSO-MDM2-probe reference. As similar with compound SM1, compound SM5 showed moderate inhibitory effect on MDM2-probe complex. The results obtained for compounds SM1 and SM5 are not statistically significant.

In the presence of compounds SM2, SM6, SM8 and SM9, the FP values of MDM2-probe complex was slightly higher than that of DMSO-MDM2-probe sample. This observation indicates that there is no inhibition in MDM2-probe complex with the existence of these compounds. Under the treatment with compounds SM3 and SM4, the FP values of MDM2-probe complex was dramatically higher than that of DMSO-MDM2-probe sample. These compounds resulted in an increase in the polarization signal of MDM2-probe complex instead of inhibition. That might be sign of a stronger binding of probe to the protein in the presence of compounds SM3 and SM4.

CHAPTER 4

CONCLUSIONS

Cancer is a disease leading higher mortality rates in world. There are many treatment strategies for cancer including surgery radiotherapy and chemotherapy. These approaches have been not sufficient to completely cure this disease. Although there are many drugs used in the treatment of cancer, still there is a need to discover novel drugs to cure cancer. A significant strategy in cancer treatment is developing drugs that is able to target specific molecular pathway of cancer.

In this thesis, we investigated the anticancer properties of ezetimibe and synthesis intermediates on three different cancer cell lines including MCF7, HeLa and LNCaP cells. These cells have different p53 and MDM2 status meaning that LNCaP cells have wild-type p53; MCF7 cells have wild-type p53 and overexpressed MDM2; HeLa cells contains wild type but not functional p53. The cytostatic and cytotoxic properties of compounds SM1-9 were investigated in these cell lines by using MTT cell proliferation assay. For most active compounds SM8 and SM9, their apoptotic effects were examined by Fluorometric Caspase 3/7 activity and Annexin-V FITC assays. Besides these purpose, the MDM2 inhibitor profile of compounds were determined by using fluorescence polarization assay.

Firstly, MTT cell viability assay is used to screen cytotoxic and cytostatic properties of compounds SM1-9. According to MTT assay results, compounds SM2, SM3, SM4 and SM6 demonstrated cytotoxic effects on three cancer cell lines at moderate to high micromolar GI_{50} values. Compounds SM2, SM3 and SM4 had more cytotoxicity on LNCaP cell line with lower GI50 values, comparing to other cells lines. Compound SM6 showed strong cytotoxic effect on all three cancer cells with closer GI_{50} values. While compounds SM1 did not show any effect on HeLa and LNCaP cells at up to 100 μM concentration, it showed cytostatic effect on MCF7 cell line. Compound SM7 was not effective on these cancer cells even up to 100 μM concentration. Compounds SM8 and SM9 had cytostatic properties on MCF, HeLa and LNCaP cell lines with low micro molar GI_{50} values. Due to these results, compounds SM8 and SM9 were selected to examine apoptotic properties in LNCaP cell lines.

Secondly, the effects of compounds SM8 and SM9 on early and late apoptotic induction in LNCaP cells were investigated. Caspase 3/7 activity assay was used for observing late apoptotic properties of these compounds. According to results, they enhanced caspase 3/7 activities in LNCaP cells comparing to negative control cells that were treated with same amount of DMSO. Additionally, idasanutlin, a MDM2 inhibitor was found to be more effective to increase caspase activities than compounds. Idasanutlin demonstrated dose-dependent induction on caspases 3/7 activity, whereas compounds SM8 and SM9 had no dose-dependent induction on caspases 3/7 activity. The effects of these compounds on apoptotic induction was also determine by Annexin-V FITC assay. This assay demonstrated that compounds SM8 and SM9 were not effective on early apoptotic processes, but they were moderately effective on late apoptotic processes. These two apoptotic assays demonstrated that compounds SM8 and SM9 have no cytotoxic property on LNCaP cells. Cell cycle analysis assay demonstrated that compound SM9 has cytostatic activity on LNCaP cells having wild-type p53. It affected on G1 phase of LNCaP cells. The result of this assay is correlated with MTT results of compound SM9.

In the final part of the thesis, MDM2 inhibitory properties of compounds SM1-9 were investigated by using fluorescence polarization assay. According to this assay results, compounds SM8 and SM9 having most antiproliferative activity showed no inhibitory properties on MDM2 protein. But compounds SM1 and SM5 demonstrated slight inhibition on MDM2- FAMprobe complex.

Table 4.1. The LogP, Log S and docking results of compounds SM1-9.

Compound	Log P	LogS	Docking (kcal/mol)
SM1	5.43	-8.06	**-8.7**
SM2	4.6	-5.83	**-8.9**
SM3	4.6	-5.83	**-9**
SM4	4.44	-5.55	**-8.8**
SM5	4.72	-6.2	**-9.3**
SM6	6.23	-8.62	**-8.8**
SM7	8.26	-11.23	**-8.6**
SM8	5.97	-8.72	**-9.1**
SM9	7.48	-9.52	**-9.1**
Pazopanip.HCl	3.82	-6.08	
İdasanutlin	7	-9.07	

Lipophilicity and solubility of a compound is important for drug discovery. Because these are the physical characteristics of compounds that are used for evaluating drug properties. Log P value is partition coefficient that is utilized as a measure for hydrophobicity and lipophilicity of drug candidates. Log S value is used for a measure of solubility of drug candidates in water. Solubility of compound is important for its adsorption and distribution features.

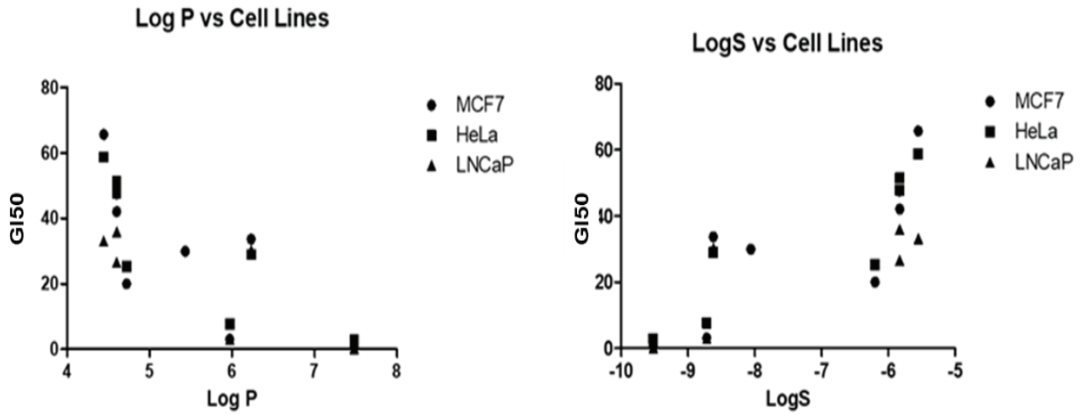

Figure 4.1. Correlation of Log P and Log S values of compounds SM1-9 compared to their GI_{50} values in MCF7, HeLa and LNCAP cell lines.

According Log P values in table 4.1 and figure 4.1, compounds having Log P values equal or larger than 6, were the most effective compounds with low GI_{50} values. It seems that Log P values lower than 6 may not produce significant antiproliferative activity in these cells. With these observations, it is proposed that more lipophilic compounds have more efficiency on cancer lines. Compound SM7 is an exception for this generalization. Hence, it can be concluded that Log P values should be higher than 6, but lower than 8.

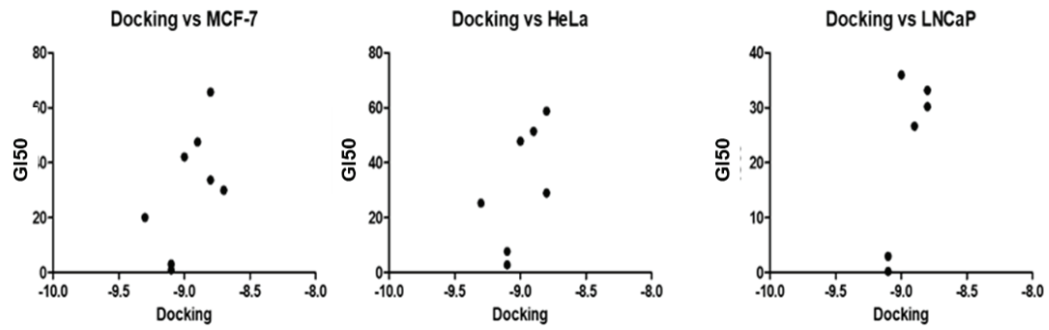

Figure 4.2. The distribution of compounds SM1-9 with GI50 values in MCF7, HeLa and LNCaP cell lines depending on their docking values.

As seen in table 4.1 and figure 4.1, compounds having higher negative Log S values were the most effective activity on MCF7 and HeLa cell lines with low GI50 values. Although Log S values of the compounds correlates mostly between -8 to -11 for stronger (or superior) antiproliferative activity. Moderate antiproliferative actrivities can be seen for Log S values between -6 to -8.

According to docking scores in table 4.1 and figure 4.2, compounds SM3, SM5, SM8 and SM9 have better docking score values than others. Better docking values demonstrates that these compounds have higher affinity for MDM2 protein. Compounds SM8 and SM9 are more effective in MCF7, HeLa and LNCaP cell lines at low micro molar concentrations. Besides, compounds SM8 and SM9 have cytostatic activity on three cancer cell lines, it was expected that they would be MDM2 inhibitor due to better docking scores. By inhibiting MDM2 –p53 probe complex, they would activate p53 to induce cell cycle arrest. However, fluorescence polarization assay results for compounds SM8 and SM9 showed that these compounds have not MDM2 inhibitor properties at 40 μM concentration. Interestingly, compounds SM1 and SM5 showed moderate inhibitory effects on MDM2 protein and MDM2-p53 probe complex. But compound SM1 had no antiproliferative activity on HeLa and LNCaP cells, whereas it had cytostatic activity on MCF7 cells with 29.95 μM.

REFERENCES

1. Blackadar, C.B., *Historical review of the causes of cancer.* World J Clin Oncol, 2016. **7**(1): p. 54-86.

2. Sung, H., et al., *Global Cancer Statistics 2020: GLOBOCAN Estimates of Incidence and Mortality Worldwide for 36 Cancers in 185 Countries.* CA Cancer J Clin, 2021. **71**(3): p. 209-249.

3. Takeshima, H. and T. Ushijima, *Accumulation of genetic and epigenetic alterations in normal cells and cancer risk.* NPJ Precis Oncol, 2019. **3**: p. 7.

4. Hanahan, D. and R.A. Weinberg, *The Hallmarks of Cancer.* Cell, 2000. **100**(1): p. 57-70.

5. Fouad, Y.A. and C. Aanei, *Revisiting the hallmarks of cancer.* American journal of cancer research, 2017. **7**(5): p. 1016-1036.

6. Soussi, T., *The history of p53. A perfect example of the drawbacks of scientific paradigms.* EMBO reports, 2010. **11**(11): p. 822-826.

7. Soussi, T., *Analysis of p53 Gene Alterations in Cancer: A Critical View*. 2007, Springer Netherlands. p. 255-292.

8. Kruiswijk, F., C.F. Labuschagne, and K.H. Vousden, *p53 in survival, death and metabolic health: a lifeguard with a licence to kill.* Nat Rev Mol Cell Biol, 2015. **16**(7): p. 393-405.

9. Moll, U.M. and O. Petrenko, *The MDM2-p53 interaction.* Mol Cancer Res, 2003. **1**(14): p. 1001-8.

10. Anderson, E.A.a.C.W., *Post-translational modifications and activation of p53 by genotoxic stresses.* Eur. J. Biochem, 2001. **268**: p. 2764±2772.

11. Zonggang Che1, H.S., Wenjing Yao3, Bei Lu4, Qiqing Han1, *Role of post-translational modifications in regulation of tumor suppressor p53 function.*

12. Levine, A.J., W. Hu, and Z. Feng, *The P53 pathway: what questions remain to be explored?* Cell Death Differ, 2006. **13**(6): p. 1027-36.

13. el-Deiry, W.S., et al., *WAF1, a potential mediator of p53 tumor suppression.* Cell, 1993. **75**(4): p. 817-25.

14. Luo, Y., et al., *Blocking CHK1 Expression Induces Apoptosis and Abrogates the G2 Checkpoint Mechanism.* Neoplasia, 2001. **3**(5): p. 411-419.

15. Chen, J., *The Cell-Cycle Arrest and Apoptotic Functions of p53 in Tumor Initiation and Progression.* Cold Spring Harb Perspect Med, 2016. **6**(3): p. a026104.

16. Gatz, S.A. and L. Wiesmüller, *p53 in recombination and repair.* Cell Death & Differentiation, 2006. **13**(6): p. 1003-1016.

17. Barboza, J.A., et al., *p21 delays tumor onset by preservation of chromosomal stability.* Proceedings of the National Academy of Sciences, 2006. **103**(52): p. 19842-19847.

18. Johnstone, R.W., A.A. Ruefli, and S.W. Lowe, *Apoptosis.* Cell, 2002. **108**(2): p. 153-164.

19. Lakin, N.D. and S.P. Jackson, *Regulation of p53 in response to DNA damage.* Oncogene, 1999. **18**(53): p. 7644-7655.

20. Williams, A.B. and B. Schumacher, *p53 in the DNA-Damage-Repair Process.* Cold Spring Harb Perspect Med, 2016. **6**(5).

21. Mulay, S.R., et al., *MDM2 (murine double minute-2) links inflammation and tubular cell healing during acute kidney injury in mice.* Kidney International, 2012. **81**(12): p. 1199-1211.

22. Iwakuma, T. and G. Lozano, *MDM2, an introduction.* Mol Cancer Res, 2003. **1**(14): p. 993-1000.

23. Chene, P., *Inhibiting the p53-MDM2 interaction: an important target for cancer therapy.* Nat Rev Cancer, 2003. **3**(2): p. 102-9.

24. Moll, U.M. and A. Zaika, *Disrupting the p53-mdm2 interaction as a potential therapeutic modality.* Drug Resist Updat, 2000. **3**(4): p. 217-221.

25. Nag, S., et al., *The MDM2-p53 pathway revisited.* J Biomed Res, 2013. **27**(4): p. 254-71.

26. Vassilev, L.T., *MDM2 inhibitors for cancer therapy.* Trends Mol Med, 2007. **13**(1): p. 23-31.

27. Schon, O., et al., *Molecular Mechanism of the Interaction between MDM2 and p53.* Journal of Molecular Biology, 2002. **323**(3): p. 491-501.

28. O'Keefe, K., H. Li, and Y. Zhang, *Nucleocytoplasmic shuttling of p53 is essential for MDM2-mediated cytoplasmic degradation but not ubiquitination.* Molecular and cellular biology, 2003. **23**(18): p. 6396-6405.

29. Qin, J.J., et al., *Natural product MDM2 inhibitors: anticancer activity and mechanisms of action.* Current medicinal chemistry, 2012. **19**(33): p. 5705-5725.

30. Chen, L., et al., *Synergistic activation of p53 by inhibition of MDM2 expression and DNA damage.* Proceedings of the National Academy of Sciences, 1998. **95**(1): p. 195-200.

31. Zhang, Z., et al., *Novel MDM2 p53-independent functions identified through RNA silencing technologies.* Ann N Y Acad Sci, 2005. **1058**: p. 205-14.

32. Nayak, S.K., et al., *p53-Mdm2 Interaction Inhibitors as Novel Nongenotoxic Anticancer Agents.* Curr Cancer Drug Targets, 2018. **18**(8): p. 749-772.

33. Secchiero, P., et al., *Recent advances in the therapeutic perspectives of Nutlin-3*. Curr Pharm Des, 2011. **17**(6): p. 569-77.

34. Neochoritis, C., et al., *p53–MDM2 and MDMX Antagonists*. 2014. p. 167-187.

35. Tisato, V., et al., *MDM2/X inhibitors under clinical evaluation: perspectives for the management of hematological malignancies and pediatric cancer.* Journal of Hematology & Oncology, 2017. **10**(1).

36. Khurana, A. and D.A. Shafer, *MDM2 antagonists as a novel treatment option for acute myeloid leukemia: perspectives on the therapeutic potential of idasanutlin (RG7388).* Onco Targets Ther, 2019. **12**: p. 2903-2910.

37. Ding, Q., et al., *Discovery of RG7388, a potent and selective p53-MDM2 inhibitor in clinical development.* J Med Chem, 2013. **56**(14): p. 5979-83.

38. Wang, S., et al., *SAR405838: an optimized inhibitor of MDM2-p53 interaction that induces complete and durable tumor regression.* Cancer Res, 2014. **74**(20): p. 5855-65.

39. de Weger, V.A., et al., *A phase I study of the HDM2 antagonist SAR405838 combined with the MEK inhibitor pimasertib in patients with advanced solid tumours.* Br J Cancer, 2019. **120**(3): p. 286-293.

40. Yu, M., et al., *Discovery of Potent and Simplified Piperidinone-Based Inhibitors of the MDM2-p53 Interaction.* ACS Med Chem Lett, 2014. **5**(8): p. 894-9.

41. Rew, Y. and D. Sun, *Discovery of a small molecule MDM2 inhibitor (AMG 232) for treating cancer.* J Med Chem, 2014. **57**(15): p. 6332-41.

42. Kang, M.H., et al., *Initial Testing (Stage 1) of MK-8242-A Novel MDM2 Inhibitor-by the Pediatric Preclinical Testing Program.* Pediatr Blood Cancer, 2016. **63**(10): p. 1744-52.

43. Pairawan, S., et al., *First in class dual MDM2/MDMX inhibitor ALRN-6924 enhances antitumor efficacy of chemotherapy in TP53 wild-type hormone receptor-positive breast cancer models.* Breast Cancer Res, 2021. **23**(1): p. 29.

44. Ding, K., et al., *Structure-Based Design of Spiro-oxindoles as Potent, Specific Small-Molecule Inhibitors of the MDM2−p53 Interaction.* Journal of Medicinal Chemistry, 2006. **49**(12): p. 3432-3435.

45. Hammersley, D. and M. Signy, *Ezetimibe: an update on its clinical usefulness in specific patient groups.* Ther Adv Chronic Dis, 2017. **8**(1): p. 4-11.

46. Kummar, S., et al., *Drug development in oncology: classical cytotoxics and molecularly targeted agents.* British Journal of Clinical Pharmacology, 2006. **62**(1): p. 15-26.

47. Verheijen, R.B., et al., *Clinical Pharmacokinetics and Pharmacodynamics of Pazopanib: Towards Optimized Dosing.* Clinical Pharmacokinetics, 2017. **56**(9): p. 987-997.

48. Natarajan, U., et al., *Cell Cycle Arrest and Cytotoxic Effects of SAHA and RG7388 Mediated through p21WAF1/CIP1 and p27KIP1 in Cancer Cells.* Medicina, 2019. **55**(2): p. 30.

49. Natarajan, U., et al., *Cell Cycle Arrest and Cytotoxic Effects of SAHA and RG7388 Mediated through p21(WAF1/CIP1) and p27(KIP1) in Cancer Cells.* Medicina (Kaunas), 2019. **55**(2).